THE JOURNAL OF PHYSICAL CHEMISTRY A

Article

Oxazine Ring-Related Vibrational Modes of Benzoxazine Monomers Using Fully Aromatically Substituted, Deuterated, N Isotope Exchanged and Oxazine-Ring-Substituted Compounds and Theoretical Calculation

Lu Han, Daniela Iguchi, Phwey S. Gil, Tyler Heyl, Victoria M Sedwick, Carlos R. Arza, Seishi Ohashi, Daniel J. Lacks, and Hatsuo Ishida

J. Phys. Chem. A, **Just Accepted Manuscript** • DOI: 10.1021/acs.jpca.7b05249 • Publication Date (Web): 27 Jul 2017

ACS Publications

The Journal of Physical Chemistry A is published by the American Chemical Society. 1155 Sixteenth Street N.W., Washington, DC 20036

Oxazine Ring-related Vibrational Modes of Benzoxazine Monomers Using Fully Aromatically Substituted, Deuterated, ^{15}N Isotope Exchanged and Oxazine-ring-substituted Compounds and Theoretical Calculation

Lu Han[1], Daniela Iguchi[1], Phwey Gil[2], Tyler Heyl[1], Victoria M. Sedwick[1], Carlos R. Arza[1], Seishi Ohashi[1], Daniel J. Lacks[2], Hatsuo Ishida[1]*

[1]Department of Macromolecular Science and Engineering, Case Western Reserve University,

[2]Department of Chemical and Biomolecular Engineering, Case Western Reserve University,

Cleveland, OH, 44106, United States.

*Corresponding Author: E-mail: hxi3@cwru.edu

ABSTRACT

Polymerization of benzoxazine resins is indicated by the disappearance of a 960-900 cm^{-1} band in infrared spectroscopy (IR). Historically, this band was assigned to the C-H out-of-plane bending of the benzene to which the oxazine ring is attached. This study shows that this band is a mixture of the O-C_2 stretching of the oxazine ring and the phenolic ring vibrational modes. Vibrational frequencies of 3-phenyl-3,4-dihydro-2*H*-benzo[e][1,3]oxazine (**PH-a**) and 3-(*tert*-butyl)-3,4-dihydro-2*H*-benzo[e][1,3]oxazine (**PH-t**) are compared with isotope-exchanged and all-substituted compounds. Deuterated benzoxazine monomers, ^{15}N-isotope exchanged benzoxazine monomers, and all-substituted benzoxazine monomers without aromatic C-H groups are synthesized and studied meticulously. The various isotopic-exchanges involved deuteration around the benzene ring of phenol, selective deuteration of each CH_2 in the O-*CH_2*-N (2) and N-*CH_2*-Ar (4) positions on the oxazine ring, or simultaneous deuteration of both positions. The chemical structures were confirmed by ^{1}H nuclear magnetic resonance spectroscopy (^{1}H NMR). The IR and Raman spectra of each compound are compared. Further analysis of ^{15}N isotope-exchanged PH-a indicates the influence of the nitrogen isotope on the band position, both experimentally and theoretically. This finding is important for polymerization studies of benzoxazines that utilize vibrational spectroscopy.

1. INTRODUCTION

Polybenzoxazine is a relatively new and commercialized thermoset resin obtained by polymerizing 1,3-benzoxazine. Recently, polybenzoxazine received much attention because of their many unique and desirable properties, such as near-zero shrinkage upon polymerization,[1,2] low flammability,[3] lower surface free energy than polytetrafluoroethylene without having fluorine atoms,[4,5] extremely flexible molecular design capability,[6-11] which even allows the use of phenols and amines from natural renewable resources,[12] and other excellent mechanical[13-15] and thermal properties.[16-17]

Benzoxazines are characterized by a broad and intense band at 960-900 cm^{-1} in the FT-IR spectrum. This band gradually disappears when benzoxazine is heated to the polymerization temperature. For fully polymerized samples, this band completely disappears.[7,18] It has been reported by Dunkers and Ishida that the disappearance of this band does not exactly coincide, but that there is a time lag between the intensity change of the 1498 cm^{-1} band (which is directly associated with the polymerization) and the band of current interest near 960-900 cm^{-1}.[19,20] While the circumstantial evidence clearly points to the strong association of the 960-900 cm^{-1} band with benzoxazine polymerization, the nature of this band has not been well understood. Historically, this band of 1,3-benzoxazine was assigned to the C-H out-of-plane bending vibrations of benzene to which the oxazine is attached. Since the band assignment of this mode in early days of benzoxazine research many years ago, no rigorous effort was made to understand this mode in detail despite its very important role in polymerization studies of benzoxazine resin. Therefore, the goal of this study is to understand the nature of this band by systematically studying the FT-IR and Raman spectra of the compounds specifically designed to answer questions related to the group that is involved and nature of the vibration.

Benzoxazines are usually synthesized by one-pot Mannich condensation of phenol, amine and formaldehyde.[21] Various benzoxazine monomers can be synthesized by using different phenolic derivatives and primary amines, which are commercially available. To selectively substitute the oxazine ring, however, there is a limitation for one-pot synthesis. In order to selectively substitute or deuterate the 2-position of the oxazine ring, 2-step synthesis should be conducted by starting with *ortho*-hydroxyl substituted benzaldehyde.[22-23] By using different benzaldehyde or formaldehyde, different oxazine-substituted benzoxazine monomers can be synthesized. On the other hand, 4 position deuterated benzoxazine can be obtained by hydrolyzing the all deuterated benzoxazine,[24] followed by closing the ring using normal paraformaldehyde.

The approaches taken in the current paper can be largely classified into two steps. First, in order to test if the band is directly from the aromatic C-H groups, a series of fully aromatically substituted benzoxazines were designed and synthesized. Two benzoxazine monomers, bis- and tris-oxazine as shown below in Figure 1, are designed to evaluate the role of the aromatic C-H on the benzoxazine modes. If the band of interest is due to the aromatic C-H, these monomers should not show this characteristic band. Although **PG-a** and **PG-anis** are the same with respect to the substitution structure, it was nonetheless synthesized to perturb the overlapped vibrational bands.

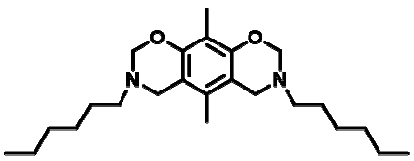

25DMR-h

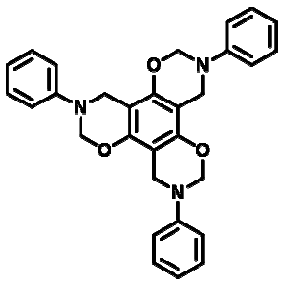

PG-a

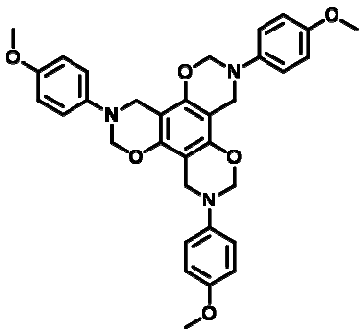

PG-anis

Figure 1. Chemical structure of all-substituted benzoxazines.

Isotopic substitution is a useful technique to assign FT-IR or Raman bands because isotopically substituted molecules are different from the unsubstituted molecule only by weight but not the electronic structure, leading to different vibrational frequencies from the same vibrational modes.[25] **PH-a-phenol-d_4**, shown in Figure 2, was designed to further evaluate if the characteristic mode is aromatic related.

The second goal of the current paper is to examine, if the band of current interest is not aromatic C-H related, then which group of the oxazine it is most strongly related to. Compounds **PH-a-2oxazine-d_2**, **PH-a-4oxazine-d_2** and **PH-a-oxazine-d_4**, are designed to evaluate if the band is related to oxazine 2, 4 position CH_2. By using symmetric and asymmetric deuteration, the specific position of the CH_2 that is related to the band can be examined. Furthermore, if the band is related to the skeletal oxazine ring mode rather than oxazine CH_2 modes, the position of the vibration, either O-C-N or N-C-Ar can be evaluated.

PH-d-a was designed to study whether the modes are associated with aniline part.

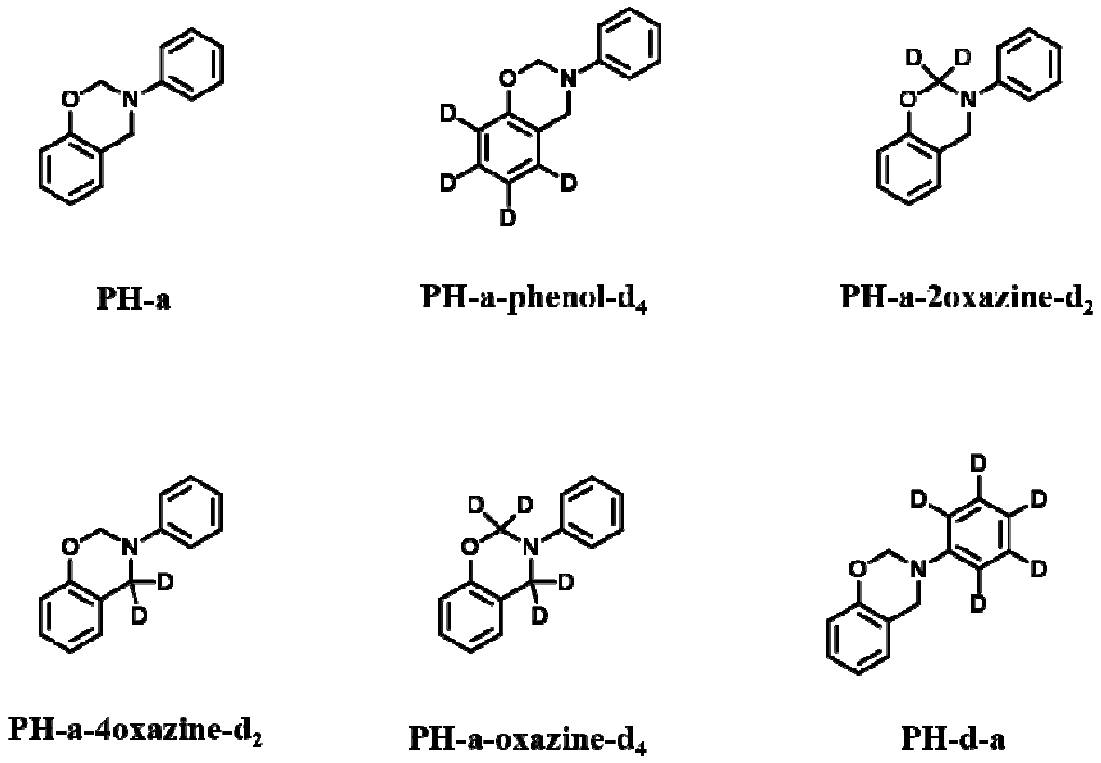

Figure 2. Chemical structure of **PH-a** series.

The following four compounds (shown in Figure 3) are the corresponding *tert*-amine versions of the monomers shown above. By using these compounds, the overlapped aromatic amine proton information can be further eliminated. Although some information obtained from the aniline-series and *tert*-amine series are redundant, it is nonetheless useful to make sure that the information obtained is reproducible.

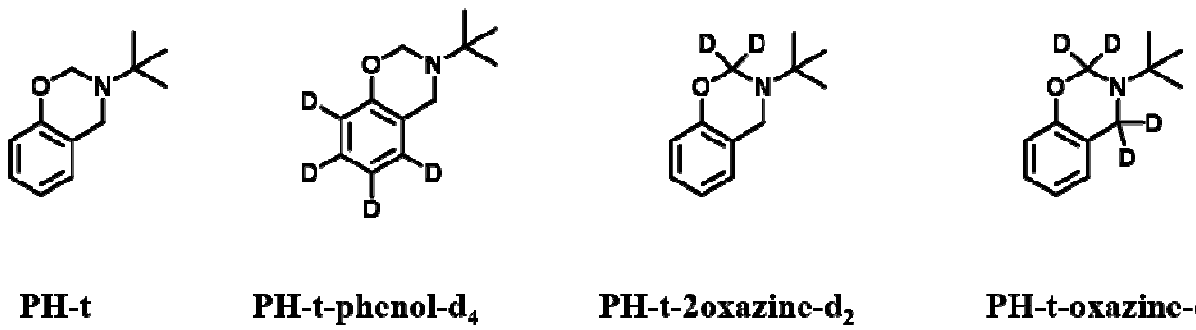

Figure 3. Chemical structure of **PH-t** series.

^{15}N-exchanged PH-a monomer, **PH-a-^{15}N**, will further allow if the characteristic mode is related to the N-C group or Ar-O/Ar-C groups.

Finally, by changing the substitution position of methyl group on the oxazine ring (shown in Figure 4.), further strong evidence can be obtained if the band belongs either to the N-CH_2-Ar or O-CH_2-N group and the conclusion derived from the ^{15}N-isotope compound can be verified.

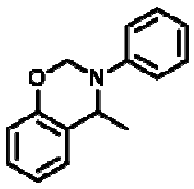

PH-a-4oxazine

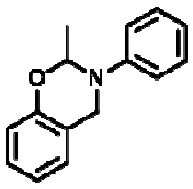

PH-a-2oxazine

Figure 4. Chemical structure of methyl group substituted benzoxazine series.

2. EXPERIMENTAL

2.1. Materials

2,5-dimethylresorcinol (95%), hexylamine (99%), phloroglucinol (≥ 99%), formaldehyde solution (37 wt. % in H_2O, contains 10-15% ethanol as stabilizer), aniline (99%), glacial acetic acid, *p*-anisidine (≥99%), salicylaldehyde (98%), paraformaldehyde-d_2 (98 atom % D), phenol (≥99%), phenol-d_6 (99 atom % D), hydrochloric acid (37.5%), distilled water, ammonium hydroxide (25% solution), *tert*-butyl amine (98%), aniline-^{15}N (98 atom % ^{15}N), 2-acetylphenol (≥98%), acetaldehyde(≥99%), and aniline-2,3,4,5,6-d_5 (98 atom % D) were purchased from

Sigma-Aldrich. Chloroform-*d* was obtained from Cambridge Isotope Laboratories, Inc. Paraformaldehyde (96%) was obtained from Acros Organics. Magnesium sulfate anhydrous, sodium hydroxide, toluene (99.9%), ethanol (200 proof), hexane (4.2% various methylpentanes), ethyl acetate, acetone, formic acid (88%), chloroform (99.9%), dichoromethane (99.9%), and diethyl ether (99.9%) were purchased from Fisher Scientific.

2.2. Characterization

^{1}H nuclear magnetic resonance (NMR) spectra were acquired on a Varian Oxford AS600 at a proton frequency of 600 MHz. The average number of transients for ^{1}H measurement was 64. A relaxation time of 10 s was used for the integrated intensity determination of ^{1}H NMR spectra. Fourier transform infrared (FT-IR) spectra were obtained using a Bomem Michelson MB100 FTIR spectrometer, which was equipped with a deuterated triglycine sulfate (DTGS) detector and a dry air purge unit. Coaddition of 64 scans was recorded at a resolution of 4 cm^{-1}. The intensity of the strongest absorption band was controlled to 0.7-1 for accuracy, by changing the thickness of the film casted on the KBr plate.

2.3. Synthesis

2.3.1. Synthesis of 3,7-dihexyl-5,10-dimethyl-3,4,7,8-tetrahydro-2*H*,6*H*-benzo[1,2-e:5,4-e']bis([1,3]oxazine) (abbreviated as 25DMR-h)

Toluene (5 mL) was added to a mixture of 2, 5-dimethylresorcinol (0.100 g, 0.72 mmol), paraformaldeyde (0.109 g, 3.62 mmol) and hexylamine (0.147 g, 1.45 mmol) in a 15 mL round bottom flask. The mixture was magnetically stirred for 6 h under reflux. The completed reaction product was washed with 1N NaOH three times and water three times. The product was dried

over magnesium sulfate anhydrous overnight. The solution was filtered to remove the salt. After drying the filtrate, the product was dried in a vacuum oven to obtain a light brown powder. Yield: 73%. ^{1}H-NMR (600 MHz, $CDCl_3$, ppm): δ 0.81-0.87 (m, 6H, -C*H*$_3$), 1.23-1.32 (m, 16H, CH_2-(C*H*$_2$)$_4$- CH_3), 1.89 (s, 3H, -C*H*$_3$), 1.98 (s, 3H, -C*H*$_3$), 2.69 (t, 4H, N-C*H*$_2$-(CH2)$_4$), 3.83 (s, 4H, Ar-C*H*$_2$-N), 4.76 (s, 4H, N-C*H*$_2$-O).

2.3.2. Synthesis of 3,7,11-triphenyl-3,4,7,8,11,12-hexahydro-2*H*,6*H*,10*H*-benzo[1,2-e:3,4-e':5,6-e'']tris([1,3]oxazine) (abbreviated as PG-a)

Ethanol (5 mL) was added to a mixture of phloroglucinol (0.100 g, 0.79 mmol), formaldehyde (0.483 g, 5.95 mmol), aniline (0.222 g, 2.38 mmol) and a catalytic amount of glacial acetic acid in a 15 mL round bottom flask. The mixture was magnetically stirred for 10 h at room temperature. The product precipitated from the reaction solvent and was collected by filtration. The product was dried in a vacuum oven to obtain a white powder. Yield: 74%. ^{1}H-NMR (600 MHz, $CDCl_3$, ppm): δ 4.43 (s, 6H, Ar-C*H*$_2$-N), 5.27 (s, 6H, N-C*H*$_2$-O), 6.91 (d, 3H, Ar*H*), 7.08 (d, 6H, Ar*H*), 7.24 (t, 6H, Ar*H*).

2.3.3. Synthesis of 3,7,11-tris(4-methoxyphenyl)-3,4,7,8,11,12-hexahydro-2*H*,6*H*,10*H*-benzo[1,2-e:3,4-e':5,6-e'']tris([1,3]oxazine) (abbreviated as PG-anis)

Ethanol (5 mL) was added to a mixture of phloroglucinol (0.100 g, 0.79 mmol), formaldehyde (0.483 g, 5.95 mmol), *p*-anisidine (0.293 g, 2.38 mmol) and a catalytic amount of glacial acetic acid in a 15 mL round bottom flask. The mixture was magnetically stirred for 8 h at room temperature. The product precipitated from the reaction solvent and collected by filtration. The product was dried in a vacuum oven to obtain white powder. Yield: 92%. ^{1}HNMR (600 MHz,

$CDCl_3$, ppm): δ 3.73 (s, 9H, C*H*$_3$), 4.34 (s, 6H, Ar-C*H*$_2$-N), 5.18 (s, 6H, N-C*H*$_2$-O), 6.78 (d, 6H, Ar*H*), 7.02 (d, 6H, Ar*H*).

2.3.4. Synthesis of 3-phenyl-3,4-dihydro-2*H*-benzo[e][1,3]oxazine (abbreviated as PH-a)

Toluene (3 mL), phenol (0.100 g, 1.06 mmol), aniline (0.094 g, 1.01 mmol) and paraformaldehyde (0.076 g, 2.53 mmol) were added to a 10 mL round bottom flask. The mixture was magnetically stirred and heated under reflux for 6 h. The completed reaction was washed with 1N NaOH three times and water three times. The product was dried over magnesium sulfate anhydrous. The material was purified in an alumina neutral column with hexane and ethyl acetate (9:1) as the eluent. The material was recrystallized from hexane. The product was a white crystal. Yield: 85%. ^{1}H-NMR (600MHz, $CDCl_3$, ppm): δ 4.64 (s, 2H, Ar-C*H*$_2$-N), 5.38 (s, 2H, N-C*H*$_2$-O), 6.84-6.85 (d,1H, Ar*H*), 6.90-6.92 (t, 1H, Ar*H*), 6.94-6.97 (t, 1H, Ar*H*), 7.02-7.04 (d, 1H, Ar*H*) 7.13-7.14 (m, 3H, Ar*H*), 7.27-7.30 (m, 2H, Ar*H*).

2.3.5. Synthesis of 3-phenyl-3,4-dihydro-2*H*-benzo[e][1,3]oxazine-5,6,7,8-d_4 (abbreviated as PH-a-phenol-d_4)

Toluene (3 mL), phenol-d_6 (0.100 g, 1.01 mmol), paraformaldehyde (0.072 g, 2.40 mmol), and aniline (0.089 g, 0.96 mmol) were added to a 10 mL round bottom flask. The mixture was magnetically stirred and heated under reflux for 6 h. The completed reaction was washed with 1N NaOH three times and water three times. The product was dried over magnesium sulfate anhydrous. The material was purified in an alumina neutral column with hexane and ethyl acetate (9:1) as the eluent. The material was recrystallized from hexane. The product was a white crystal. Yield: 88%. ^{1}H-NMR (600 MHz, $CDCl_3$, ppm): 4.62 (s, 2H, Ar-C*H*$_2$-N), 5.34 (s, 2H, N-C*H*$_2$-O), 6.90-6.92 (t, 1H, Ar*H*) 7.08-7.10 (d, 2H, Ar*H*), 7.23-7.26 (t, 2H, Ar*H*).

2.3.6. Synthesis of 3-phenyl-3,4-dihydro-2*H*-benzo[e][1,3]oxazine-2,2-d_2 (abbreviated as PH-a-2oxazine-d_2)

Ethanol (40 mL) was added to a mixture of salicylaldehyde (1.000 g, 8.18 mmol) and aniline (0.762 g, 8.18 mmol) in a 100 mL round bottom flask. The mixture was magnetically stirred for 2 h under reflux. After cooling to room temperature, $NaBH_4$ (1.549 g, 40.8 mmol) was added once an hour, three times. The solution was precipitated in water and dried to yield a white powder 2-((phenylamino)methyl)phenol (**2-pamp**). The powder was dried in vacuum oven to eliminate the remaining water. Yield: 94%.

Toluene (3 mL), **2-pamp** (0.467 g, 2.34 mmol), and paraformaldehyde-d_2 (0.093 g, 2.93 mmol) were added to a 10 mL round bottom flask. The mixture was magnetically stirred and heated under reflux for 6 h. The completed reaction was washed with 1N NaOH three times and water three times. The product was dried over magnesium sulfate anhydrous. The material was purified in an alumina neutral column with hexane and ethyl acetate (9:1) as the eluent. The material was recrystallized from hexane. The product produced was a white crystal. Yield: 83%. ^{1}H-NMR (600 MHz, $CDCl_3$, ppm): δ 4.62 (s, 2H, Ar-C*H*$_2$-N), 6.79-6.80 (d, 1H, Ar*H*), 6.86-6.88 (t, 1H, Ar*H*), 6.91-6.93 (t, 1H, Ar*H*), 6.99-7.01 (d, 1H, Ar*H*), 7.09-7.11 (t, 3H, Ar*H*), 7.23-7.26 (t, 2H, Ar*H*).

2.3.7. Synthesis of 3-phenyl-3,4-dihydro-2*H*-benzo[e][1,3]oxazine-2,2,4,4-d_4 (abbreviated as PH-a-oxazine-d_4)

Toluene (15 mL) was added to a mixture of phenol (0.500 g, 5.32 mmol), paraformaldehyde-d_2 (0.405 g, 5.00 mmol), and aniline (0.472 g, 5.10 mmol) in a 50 mL round bottom flask. The mixture was magnetically stirred and heated under reflux for 6 h. The completed reaction was

washed with 1N NaOH three times and water three times. The product was dried over magnesium sulfate anhydrous. The material was purified in an alumina neutral column with hexane and ethyl acetate (9:1) as the eluent. The material was recrystallized from hexane. The product produced was a white crystal. Yield: 85%. ^{1}H-NMR (600 MHz, $CDCl_3$, ppm): δ 6.73-6.750 (d, 1H, Ar*H*), 6.81-6.83 (t, 1H, Ar*H*), 6.94-6.96 (d, 1H, Ar*H*), 7.03-7.06 (t, 3H, Ar*H*), 7.18-7.21 (t, 2H, Ar*H*).

2.3.8. Synthesis of 3-phenyl-3,4-dihydro-2*H*-benzo[e][1,3]oxazine-4,4-d_2 (abbreviated as PH-a-4oxazine-d_2)

PH-a-oxazine-d_4 (0.500 g, 2.32 mmol) was dissolved in 25 mL of *n*-propanol, hydrochloric acid (37.5% w/w, 7.14 mL) and distilled water (3.57 mL) was added to the solution. The mixture was magnetically stirred and heated under reflux for 2 h. After cooling to 0^{o}C, 25% ammonium hydroxide (17.87 mL) was added to the solution. The mixture was magnetically stirred for 1 hour at room temperature. After extracting with ethyl acetate 3 times, a white powder 2-((phenylamino)methyl-d_2)phenol (**2-pamd$_2$p**) was obtained after drying the solvent in the vacuum oven. Yield: 95%.

Toluene (3 mL), **2-pamd$_2$p** (0.259 g, 1.29 mmol), and paraformaldehyde-d_2 (0.048 g, 1.61 mmol) were added to a 10 mL round bottom flask. The mixture was magnetically stirred and heated under reflux for 6 h. The completed reaction product was washed with 1N NaOH three times and water three times. The product was dried over magnesium sulfate anhydrous. The material was purified in an alumina neutral column with hexane and ethyl acetate (9:1) as the eluent. The material was recrystallized from hexane. The product produced was a white crystal. Yield: 82%. ^{1}H-NMR (600 MHz, $CDCl_3$, ppm): δ 5.34 (s, 2H, N-CH_2-O), 6.78-6.80 (d, 1H,

Ar*H*), 6.86-6.88 (t, 1H, Ar*H*), 6.91-6.93 (t, 1H, Ar*H*), 6.99-7.00 (d, 1H, Ar*H*), 7.08-7.11 (t, 3H, Ar*H*), 7.23-7.26 (t, 2H, Ar*H*).

2.3.9. Synthesis of 3-(phenyl-d_5)-3,4-dihydro-2*H*-benzo[e][1,3]oxazine (abbreviated as PH-d-a)

Toluene (3 mL), phenol (0.100 g, 1.06 mmol), paraformaldehyde (0.076 g, 2.53 mmol) and aniline-2,3,4,5,6-d_5 (0.099 g, 1.01 mmol) were added to a 10 mL round bottom flask. The mixture was magnetically stirred and heated under reflux for 6 h. The completed reaction was washed with 1N NaOH three times and water three times. The product was dried over magnesium sulfate anhydrous. The material was purified in an alumina neutral column with hexane and ethyl acetate (9:1) as the eluent. The material was recrystallized from hexane. The product produced was a white crystal. Yield: 90%. ^{1}H-NMR (600 MHz, $CDCl_3$, ppm): 4.66 (s, 2H, Ar-CH_2-N), 5.39 (s, 2H, N-CH_2-O), 6.83-6.85 (d, 1H, Ar*H*) 6.90-6.93 (t, 1H, Ar*H*), 7.04-7.05 (d, 1H, Ar*H*), 7.13-7.16 (t, 1H, Ar*H*).

2.3.10. Synthesis of 3-(*tert*-butyl)-3,4-dihydro-2*H*-benzo[e][1,3]oxazine (abbreviated as Ph-t)

Toluene (3 mL) was added to a mixture of phenol (0.100g, 1.06 mmol), *tert*-butyl amine (0.074 g, 1.01 mmol) and paraformaldehyde (0.076 g, 2.40 mmol) in a 10 mL round bottom flask. The mixture was magnetically stirred for 2 h under reflux. The yellowish solution was washed with 1N NaOH three times and water three times. The solution was dried over magnesium sulfate anhydrous overnight. The material was purified in an alumina neutral column with hexane as the eluent. The purified compound was a transparent liquid. Yield: 77%. ^{1}H-NMR (600 MHz,

$CDCl_3$, ppm): δ 1.22 (s, 9H, C*H*$_3$), 4.130 (s, 2H, Ar-C*H*$_2$-N), 5.00 (s, 2H, N-C*H*$_2$-O), 6.76-6.77 (d, 1H, Ar*H*), 6.85-6.87 (t, 1H, Ar*H*), 6.99-7.00 (d, 1H, Ar*H*), 7.08-7.10 (t, 1H, Ar*H*).

2.3.11. Synthesis of 3-(*tert*-butyl)-3,4-dihydro-2*H*-benzo[e][1,3]oxazine-5,6,7,8-d_4 (abbreviated as PH-t-phenol-d_4)

Toluene (3 mL) was added to a mixture of phenol-d_6 (0.100 g, 1.00 mmol), *tert*-butyl amine (0.070 g, 0.95 mmol) and paraformaldehyde (0.071 g, 2.40 mmol) in a 10 mL round bottom flask. The mixture was magnetically stirred for 2 h under reflux. The yellowish solution was washed with 1N NaOH three times and water three times. The solution was dried over magnesium sulfate anhydrous overnight. The material was purified in an alumina neutral column with hexane as the eluent. The purified compound was a transparent liquid. Yield: 78%. ^{1}H-NMR (600 MHz, $CDCl_3$, ppm): δ 1.184 (s, 9H, C*H*$_3$), 4.097 (s, 2H, Ar-C*H*$_2$-N), 4.962 (s, 2H, N-C*H*$_2$-O).

2.3.12. Synthesis of 3-(*tert*-butyl)-3,4-dihydro-2*H*-benzo[e][1,3]oxazine-2,2-d_2 (abbreviated as PH-t-2oxazine-d_2)

Ethanol (20 mL) was added to a mixture of salicylaldehyde (1.000 g, 8.19 mmol) and aniline (0.599 g, 8.19 mmol) in a 50 mL round bottom flask. The mixture was magnetically stirred for 2 h under reflux. After cooling to room temperature, $NaBD_4$ (1.549 g, 40.95 mmol) was added once an hour for three times. The solution was precipitated in 100 mL water by adjusting the pH to 8. Dichloromethane was used to extract the intermediate 2-((*tert*-butylamino)methyl)phenol (**2-tbamp**) from the aqueous layer three times. The solution was dried over magnesium sulfate anhydrous overnight. After filtering the salt, the filtrate was dried in a vacuum oven. A white crystal was obtained. Yield: 62%.

Toluene (3 mL), **2-tbamp** (0.200 g, 1.12 mmol), and paraformaldehyde-d_2 (0.045 g, 1.40 mmol) were added to a 10 mL round bottom flask. The mixture was magnetically stirred and heated under reflux for 2 h. The yellowish solution was washed with 1N NaOH three times and water three times. The solution was dried over magnesium sulfate anhydrous overnight. The material was purified in an alumina neutral column with hexane as the eluent. The purified compound was a transparent liquid. Yield: 77%. ^{1}H-NMR (600 MHz, $CDCl_3$, ppm): δ 1.20 (s, 9H, C*H*$_3$), 4.11 (s, 2H, Ar-C*H*$_2$-N), 6.75 (d, 1H, Ar*H*), 6.83-6.85 (t, 1H, Ar*H*), 6.95-6.97 (d, 1H, Ar*H*), 7.05-7.08 (t, 1H, Ar*H*).

2.3.13. Synthesis of 3-(*tert*-butyl)-3,4-dihydro-2*H*-benzo[e][1,3]oxazine-2,2,4,4-d_4 (abbreviated as PH-t-oxazine-d_4)

Toluene (3 mL) was added to a mixture of phenol (0.100g, 1.06 mmol), *tert*-butyl amine (0.074 g, 1.01 mmol) and paraformaldehyde-d_2 (0.081 g, 2.53 mmol) in a 10 mL round bottom flask. The mixture was magnetically stirred for 2 h under reflux. The yellowish solution was washed with 1N NaOH three times and water three times. The solution was dried over magnesium sulfate anhydrous overnight. The material was purified in an alumina neutral column with hexane as the eluent. The purified compound was a transparent liquid. Yield: 76%. ^{1}H-NMR (600 MHz, $CDCl_3$, ppm): δ 1.174 (s, 9H, C*H*$_3$), 6.72-6.73 (d, 1H, Ar*H*), 6.81-6.83 (t, 1H, Ar*H*), 6.95-6.96 (d, 1H, Ar*H*), 7.04-7.07 (t, 1H, Ar*H*).

2.3.14. Synthesis of 3-phenyl-3,4-dihydro-2*H*-benzo[e][1,3]oxazine-3-^{15}N (abbreviated as ^{15}N-PH-a)

Toluene (3 mL), phenol (0.110g, 1.12 mmol), paraformaldehyde (0.080 g, 2.66 mmol) and aniline-^{15}N (0.100 g, 1.06 mmol) were added to a 10 mL round bottom flask. The mixture was

magnetically stirred and heated under reflux for 6 h. The completed reaction product was washed with 1N NaOH three times and water three times. The product was dried over magnesium sulfate anhydrous. The material was purified in an alumina neutral column with hexane and ethyl acetate (9:1) as the eluent. The material was recrystallized from hexane. The product produced was a white crystal. Yield: 90%. ^{1}H-NMR (600 MHz, $CDCl_3$, ppm): 4.67 (s, 2H, Ar-C*H*$_2$-N), 5.40 (s, 2H, N-C*H*$_2$-O), 6.84-6.86 (d, 1H, Ar*H*) 6.91-6.94 (t, 1H, Ar*H*), 6.95-6.98 (t, 1H, Ar*H*), 7.05-7.06(d, 1H, Ar*H*), 7.14-7.16 (d, 3H, Ar*H*), 7.29-7.32 (t, 2H, Ar*H*).

2.3.15. Synthesis of 4-methyl-3-phenyl-3,4-dihydro-2*H*-benzo[e][1,3]oxazine (abbreviated as Ph-a-4oxazine)

Ethanol (20 mL) was added to a mixture of 2-acetylphenol (0.500 g, 3.67 mmol) and aniline (0.342 g, 3.67 mmol) in a 50 mL round bottom flask. The mixture was magnetically stirred for 2 h under reflux. After cooling to room temperature, $NaBH_4$ (0.695 g, 18.36 mmol) was added once an hour for three times. The solution was precipitated in water and dried to yield a white powder (2-(1-(phenylamino)ethyl)phenol (abbreviated as **2-1-pamep**). The powder was dried in a vacuum oven to get rid of the remaining water. Yield: 89%.

Toluene (3 mL), **2-1-pamep** (0.400g, 1.88 mmol), and paraformaldehyde (0.070 g, 2.34 mmol) were added to a 10 mL round bottom flask. The mixture was magnetically stirred and heated under reflux for 6 h. The completed reaction was washed with 1N NaOH three times and water three times. The product was dried over magnesium sulfate anhydrous. The material was purified in an alumina neutral column with hexane and ethyl acetate (9:1) as the eluent. The material was recrystallized from hexane. The product produced was a white crystal. Yield: 83%. ^{1}H-NMR (600 MHz, $CDCl_3$, ppm): δ 1.73-1.74 (d, 3H, CH-C*H*$_3$), 4.68-4.71 (m, 1H, C*H*-CH_3), 5.24-5.26

(d, 1H, N-CH_2-O), 5.43-5.45 (d, 1H, N-CH_2-O), 6.88-6.97 (m, 3H, Ar*H*), 7.05-7.06 (d, 1H, Ar*H*), 7.13-7.15 (m, 3H, Ar*H*), 7.27-7.30 (m, 2H, Ar*H*).

2.3.16. Synthesis of 2-methyl-3-phenyl-3,4-dihydro-2*H*-benzo[e][1,3]oxazine (abbreviated as Ph-a-2oxazine)

Toluene (3 mL), **2-pamp** (0.400 g, 2.08 mmol), and acetaldehyde (0.093 g, 2.11 mmol) were added to a 10 mL round bottom flask. The mixture was magnetically stirred and heated under reflux for 6 h. The completed reaction was washed with 1N NaOH three times and water three times. The product was dried over magnesium sulfate anhydrous. The material was purified in an alumina neutral column with hexane and ethyl acetate (9:1) as the eluent. The product produced was a viscous liquid. Yield: 83%. ^{1}H-NMR (600 MHz, $CDCl_3$, ppm): δ 1.54-1.55 (d, 3H, CH-CH_3), 4.49-4.55 (q, 2H, Ar-CH_2-N), 5.62-5.65 (q, 1H, N-C*H*-Ar), 6.80-6.82 (d, 1H, Ar*H*), 6.86-6.88 (t, 1H, Ar*H*), 6.96-7.00 (m, 2H, Ar*H*), 7.08-7.10 (d, 2H, Ar*H*), 7.12-7.14 (t, 1H, Ar*H*), 7.22-7.25 (m, 2H, Ar*H*).

2.4 Computational Calculation

The Kohn-Sham formulation of density functional theory (DFT)[26,27] with the B3LYP functional[28-31] and the 6-31G** basis set[32-33] is used. The 6-31G** basis set is used because the inclusion of polarization functions on hydrogen atom orbitals significantly improved the agreement between computed and experimental FT-IR spectra.

To carry out the vibrational analysis, the geometry of the molecule must first be optimized with the same level of theory and basis set. The crystal structure of 3-phenyl-6,8-dichloro-3,4-dihydrogen-1,3-benzoxazine (**dichlorinated PH-a**) has been reported by Liu and Gu using x-ray

diffraction (XRD) experiments.[34] This molecule was reported to take a semi-chair conformation, where the benzene-oxazine rings and the aniline rings have an interplanar angle of nearly 90°. This structure was used as the starting structure of **PH-a**, the monomer of current interest, in the geometry optimization calculations. The same initial structure was used for simulations of molecular isotopes, since molecular isotopes have nearly identical geometries.[35] Avogadro, a molecule editing software, was used to draw the initial structure of all simulated molecules.[36]

Geometry optimization and vibrational analysis were performed with Gaussian 09 software.[37,38] GaussSum3[39] was used to extract the IR and Raman spectra from the Gaussian output. Computed vibrational frequencies are often multiplied by a constant factor. The scaling partially compensates for the errors associated with the assumption of harmonic vibrational modes (whereas real vibrational modes are anharmonic) and with the electron correlation approximations of the theory. The scaling factors are empirical; they are determined by comparing experimental and calculated frequencies. To achieve this 15 strong bands from each **PH-a** and 6 **PH-a** isotopes experimental FT-IR spectra were correlated to the theoretical results obtaining the average scaling factor of 0.970 (See Table S1 in SI). This methodology is similar to how Irikura et al. determine scaling factors.[40]

Vibrational Energy Distribution Analysis 4 software (VEDA4)[41] was utilized to perform the potential energy distribution (PED) calculations. VEDA4 optimization procedure is designed so that combinations of linearly independent internal coordinates are as close as possible to the normal coordinates. VEDA4 was used to process the Gaussian output, yielding the full PED matrix for analysis.

2.5 Deconvolution of Heavily Overlapped Bands

Peakfit V4.12 (Systat Software Inc.) was used for deconvolution of heavily overlapped IR bands, in particular the band in question around 960-900 cm^{-1}. The range for curve resolving is set based on the two minimum data points close to characteristic band in FT-IR spectrum. AutoFit Peaks II Second Derivative method (Baseline: Linear, D2, total%=3.0, Smoothing%=1.00, Peak type: Spectroscopy, Gaussian * Lorentz, AutoScan: Amp%=1.50, Vary Widths, Vary shape) gave the initial peak positions. Repeated the Numerical Fitting routine until iteration is equal to 7.[42,43]

3. Results and Discussion

In this paper, we have taken two different approaches to understand the nature of the prominent IR band around 960-900 cm^{-1} which was previously assigned as the C-H out-of-plane mode of benzene ring to which oxazine is attached.

3.1 Results

3.1.1. All-substituted benzoxazine monomers

Three all-substituted benzoxazine monomers, have been synthesized according to Scheme 1. The first monomer is a bisoxazine which is abbreviated as **25DMR-h** and is derived from 2, 5-dimethylresorcinol and hexylamine. Others are trisoxazines which are abbreviated as **PG-a** or **PG-anis**. These are derived from phloroglucinol with aniline.

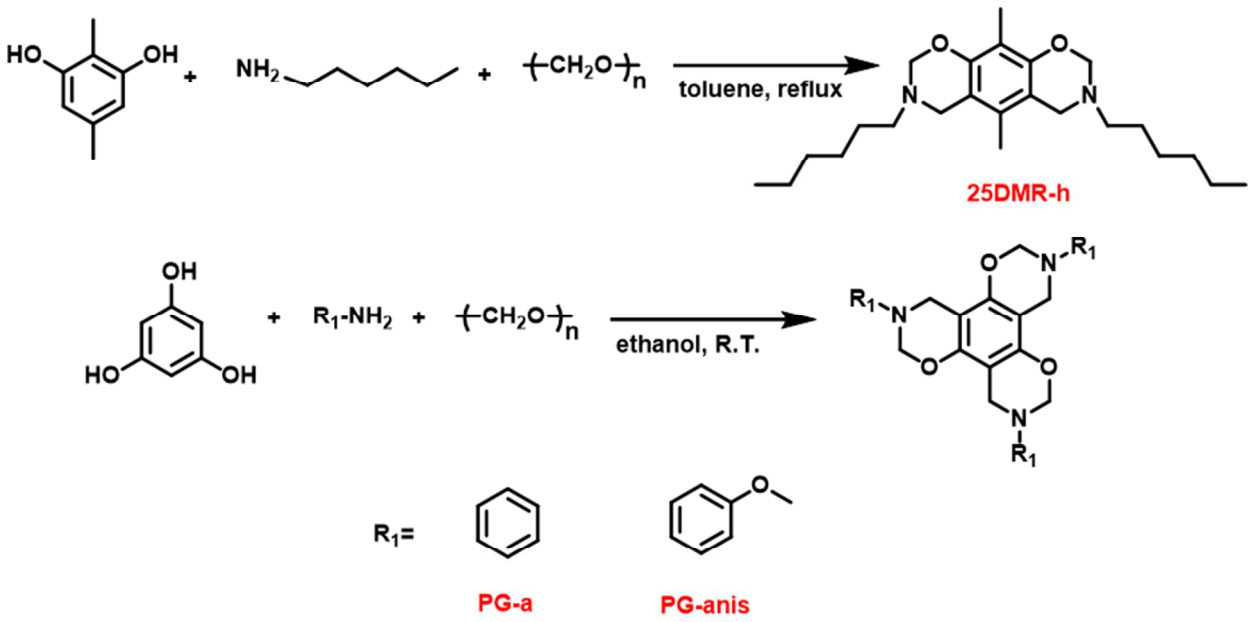

Scheme 1. Synthesis scheme of all substituted benzoxazine.

In order to verify if the synthesis was successful, ^{1}H NMR spectra of these three compounds were obtained as shown in Figure 5.

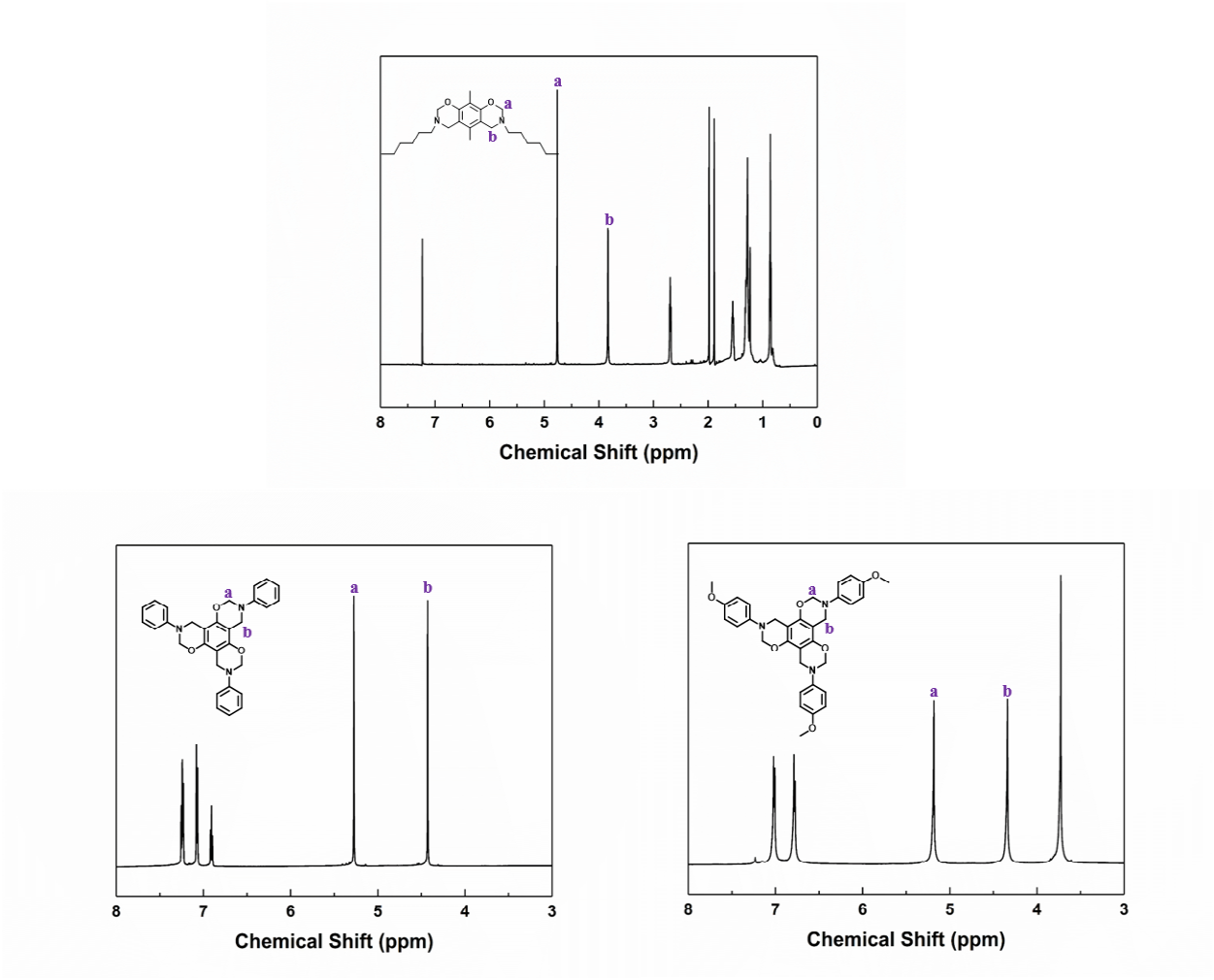

Figure 5. ^{1}H-NMR spectra for (a)**25DMR-h**, (b)**PG-a** and (c)**PG-anis** in $CDCl_3$ at room temperature

The characteristic oxazine CH_2 resonances are observed at 3.83 and 4.76 ppm for **25DMR-h**, 4.43 and 5.27 ppm for **PG-a**, and 4.34 and 5.18 ppm for **PG-anis**, indicating that the intended synthesis was successful.

The FT-IR spectra of those three fully substituted benzoxazine monomer and its heated samples are shown in Figure 6. All three monomers, **25DMR-h**, **PG-a** and **PG-anis**, show the characteristic band at 941, 948, and 936 cm^{-1}, respectively, suggesting that this mode is not

exclusively the C-H out-of-plane bending mode of the benzene ring to which the oxazine ring is attached, as historically assigned, since all three compounds lack the aromatic C-H group. The possible contribution of C-H out-of-plane bending to this band, however, cannot be excluded by this experiment. These bands completely disappear upon heat treatment at 180 ^{o}C for 2 h, strongly supporting that this characteristic mode relates to the oxazine group. Hence, it is now possible to reassign this band as oxazine ring related. It is interesting to note that this characteristic band for the all-substituted benzoxazine monomers is much shaper in comparison to the monomers with C-H groups in the ring (for example Figure 8. Left. (a)). The absence of C-H groups eliminates their contribution to the characteristic band. Thus, it is possible that this band still correlates to the C-H out-of-plane bending vibration.

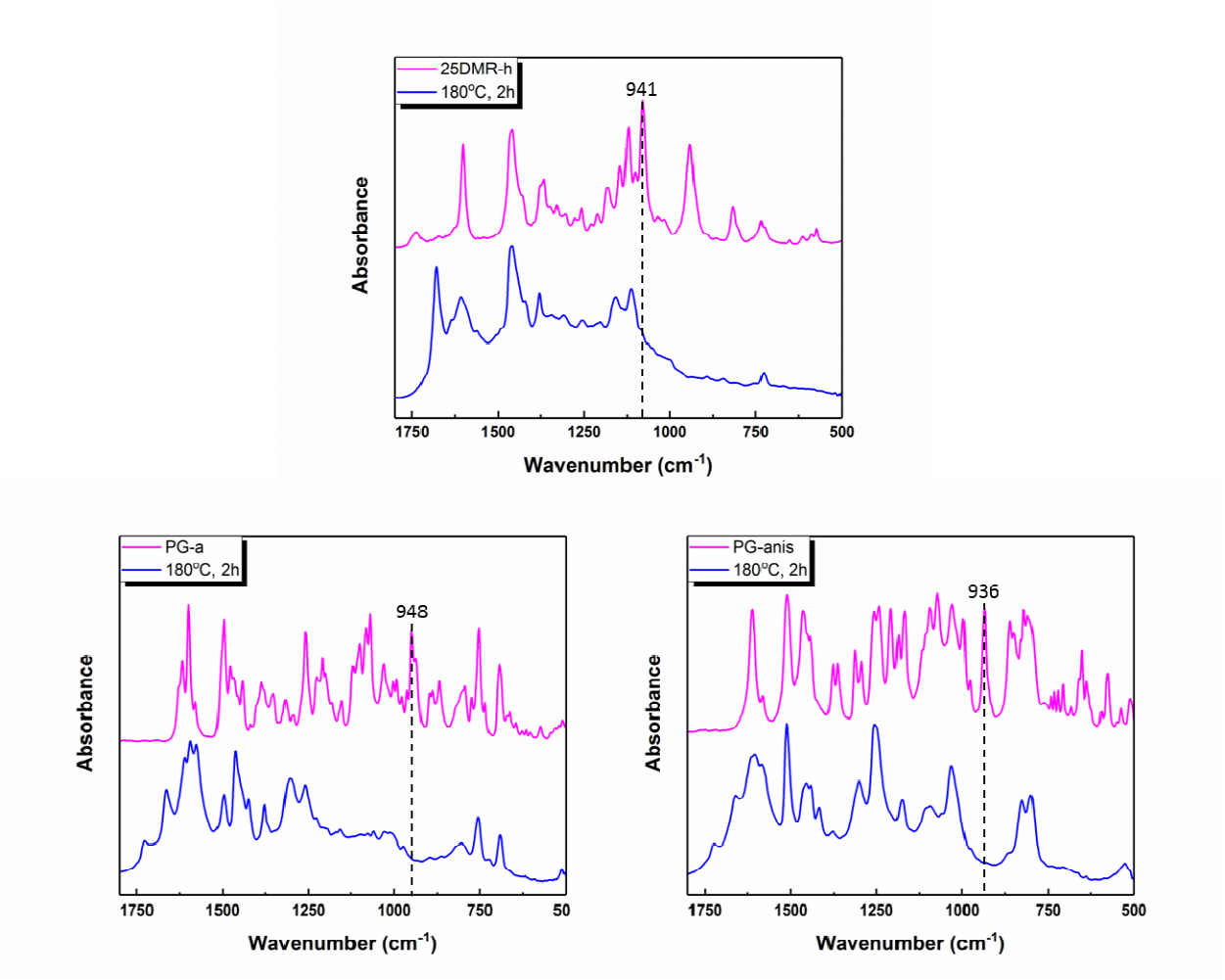

Figure 6. Comparison of FT-IR spectra of all-substituted benzoxazine monomer (top) and its corresponding polymer obtained by heating the monomer at 180°C for 2 h (bottom): (a) **25DMR-h** and its polymer; (b) **PG-a** and its polymer; (c) **PG-anis** and its polymer**.**

In order to further verify the correctness of this new reassignment, various deuterated benzoxazine monomers have been synthesized as follows.

3.1.2 Deuterium exchanged benzoxazine monomers.

Benzoxazines are often synthesized *via* one-pot Mannich condensation reaction by simply mixing phenol, amine and formaldehyde. However, this method can only be used to synthesize

benzoxazines where no distinction of 2 and 4 positions of oxazine ring is required, if substitution on the oxazine ring is desired. Thus, one-pot synthesis is used for the synthesis of **PH-x**, **PH-x-phenol-d_4, PH-x-oxazine-d_4 and PH-d-a**, as shown in Scheme 2 where x can be either a phenyl or *t*-butyl group.

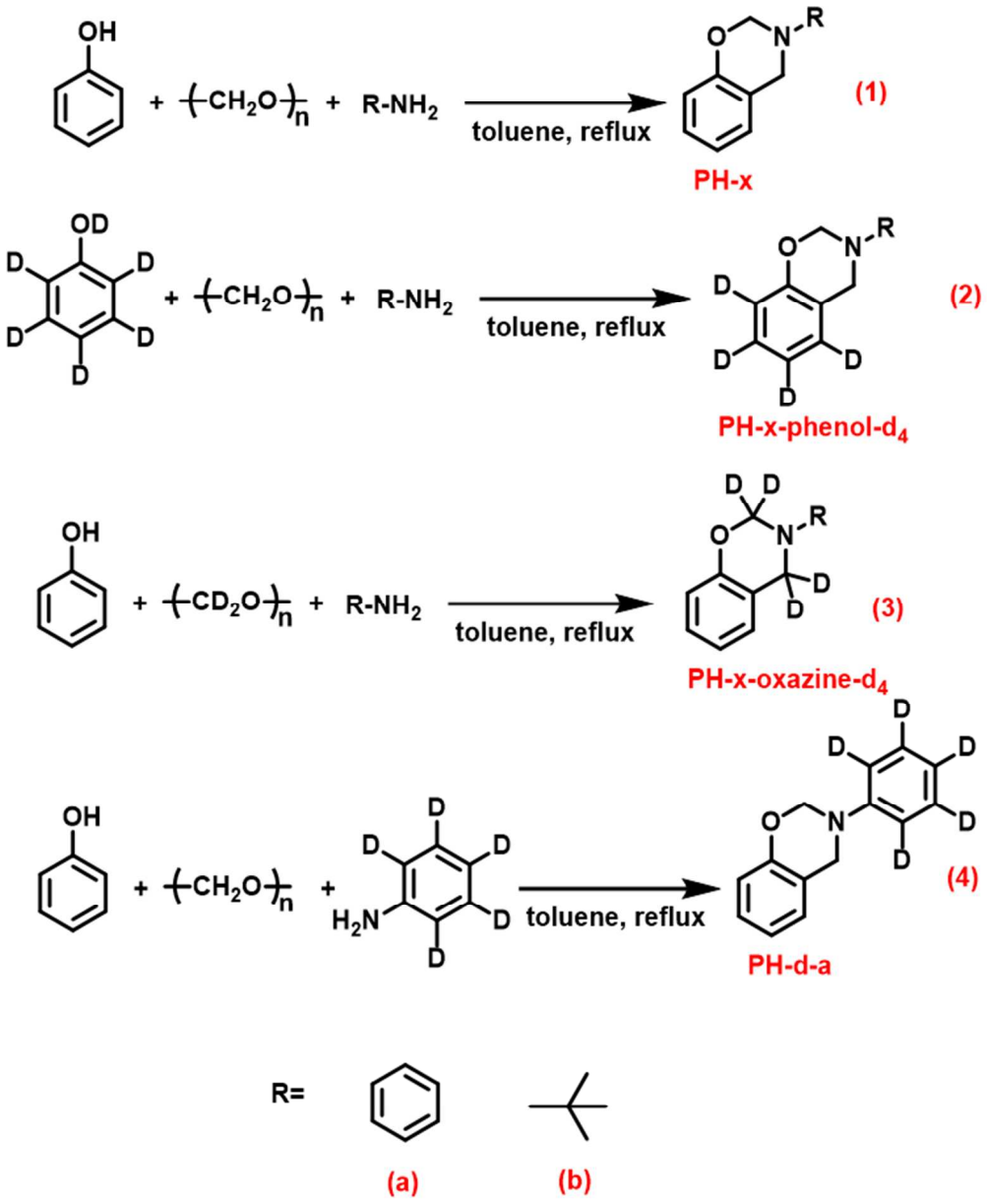

Scheme 2. Synthesis scheme of isotopes of **PH-x**, **PH-x-phenol-d$_4$**, **PH-x-oxazine-d$_4$** and **PH-d-a**.

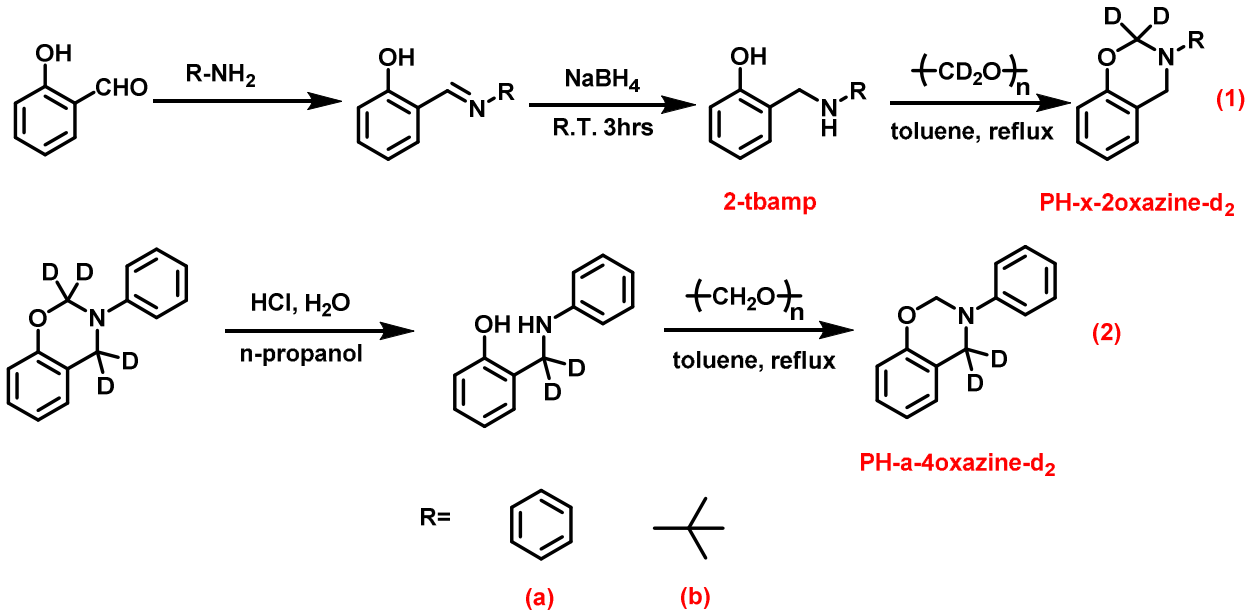

Scheme 3. Synthesis scheme of isotopes of **PH-x-2oxazine-d$_2$** and **PH-x-4oxazine-d$_2$**.

In the case of **PH-x-2oxazine-d$_2$ and PH-x-4oxazine-d$_2$** where the CH_2 groups of the oxazine group at the 2 and 4 positions, respectively, are selectively deuterated, multiple-step preparation methods as shown in Scheme 3 were adopted. For the synthesis of **PH-x-2oxazine-d$_2$** monomer, the amine was reacted with 2-hydroxybenzaldehyde, and the obtained compound was reduced by sodium borohydride. Deuterated paraformaldehyde is used to close the ring, selectively deuterating the CH_2 group at the 2 position. Total yields of 78% and 48% for **PH-a-oxazine-d$_2$** and **PH-t-oxazine-d$_2$** were obtained, respectively. The lower yield for **PH-t-oxazine-d$_2$** is due to the difficulty in precipitation of the intermediate **2-tbamp** from water. The compound was extracted from the aqueous layer. When the **PH-a** and **PH-t** series are compared, it is noted that the **PH-t** series require less reaction time because of the higher basicity of alkyl chain amine than

aromatic amine. The reaction time decreases from 6 h to 2 h. Additionally, the **PH-t** series eliminates completely the aromatic C-H signals that arise from the aromatic amine of the **PH-a** series. For the case of **PH-a-4oxazine-d_2** monomer, the reaction starts from the **PH-a-oxazine-d_4**, opening the all deuterated oxazine ring by hydrolysis, then closing the ring by normal paraformaldehyde.

In addition to the all-substituted benzoxazine monomers, the deuterium-exchanged benzene structure will also help verify if the band in question is aromatic C-H origin as previously assigned. In case the prominent band in the range of 960-900 cm^{-1} is suspected to arise from the oxazine rather than the benzene, the deuterated oxazine ring in whole or in part will help identify specific mode of the oxazine ring. The synthesis procedures adopted for each benzoxazine monomer are shown in Scheme 2.

The successful synthesis of all these monomers with high purity are supported by the ^{1}H NMR spectra shown in Figure 7. The characteristic CH_2 resonances of the oxazine ring are clearly seen at 5.38 and 4.64 ppm for **PH-a**, 5.35 and 4.62 ppm for **PH-a phenol-d_4** and 5.39 and 4.66ppm for **PH-d-a**. These two singlets became only one resonance at 4.62 ppm for **PH-a-2oxazine-d_2**, at 5.34 ppm for **PH-a-4oxazine-d_2**, and as expected, no CH_2-related resonances are seen for **PH-a-oxazine-d_4**. Exactly the same trend is observed for **PH-t** series, also strongly supporting that the expected synthesis had been successfully achieved.

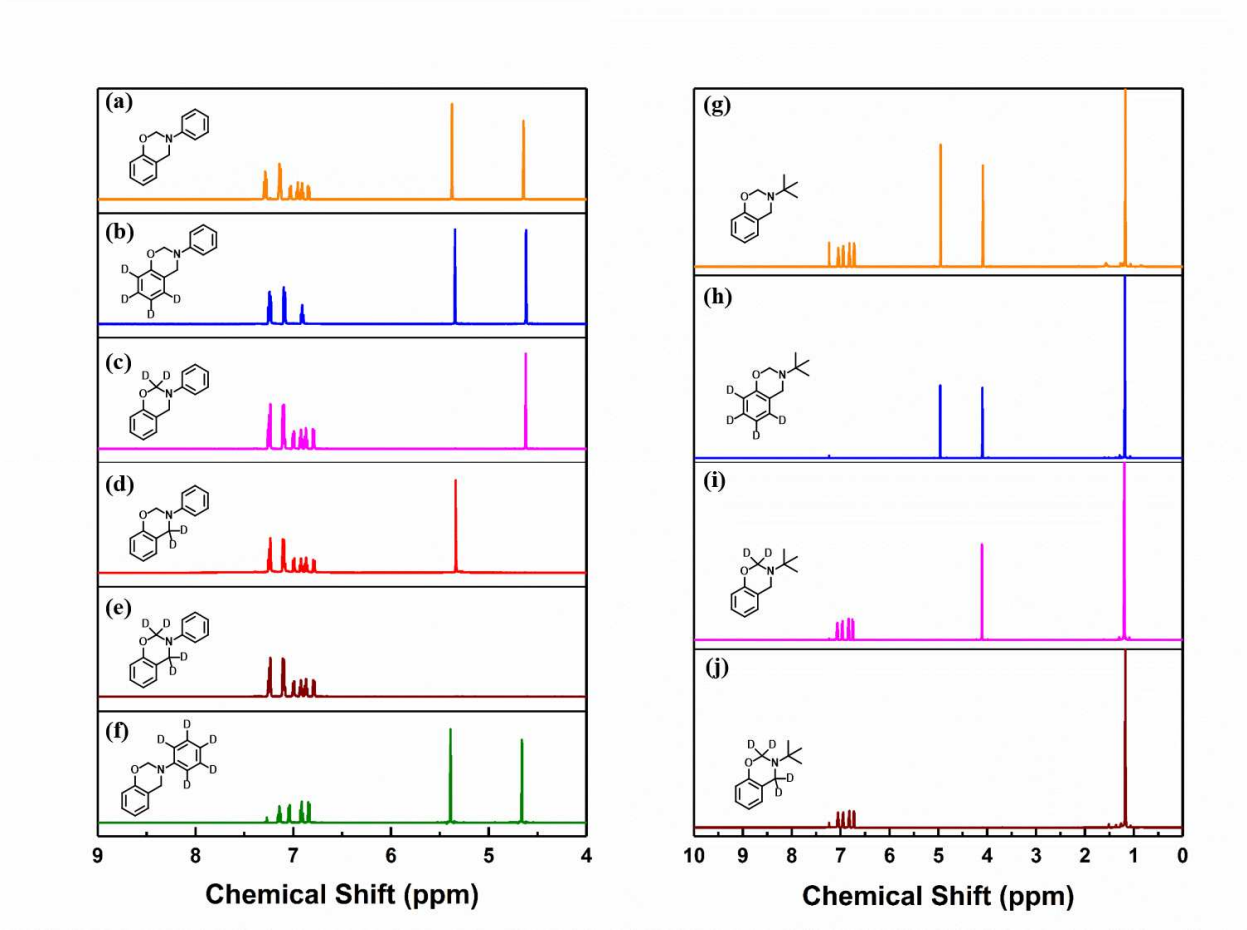

Figure 7. ^{1}H-NMR spectra for **PH-a** isotopes (left) and **PH-t** isotopes (right). (a) **PH-a**, (b) **PH-a-phenol-d$_4$**, (c) **PH-a-2oxazine-d$_2$**, (d) **PH-a-4oxazine-d$_2$**, (e) **PH-a-oxazine-d$_4$**, (f) **PH-d-a**, (g) **PH-t**, (h) **PH-t-phenol-d$_4$**, (i) **PH-t-2oxazine-d$_2$**, (j) **PH-t-oxazine-d$_4$** in $CDCl_3$ at room temperature.

The FT-IR spectra of all six compounds of the **PH-a** series and four of the **PH-t** series are shown in Figure 8. The characteristic band in question did not significantly change its position for any compound. Therefore, it is concluded that the band of interest should not be exclusively assigned to either the aromatic C-H or the oxazine CH_2 groups. It is interesting to note that the rather large frequency shift, from around 940 cm^{-1} to 915 cm^{-1}, is observed when the substituent on the

oxazine ring changed from a heavy phenyl group to a lighter *t*-butyl group. Therefore, it is now hypothesized that this mode in question may be of the oxazine skeletal mode.

Special attention should be paid to the band shift from around 753 cm^{-1} to 582 cm^{-1} in **PH-t** series. The band can be assigned to the C-H out-of-plane bending of the aromatic group due to the substitution of C-H by C-D.[44]

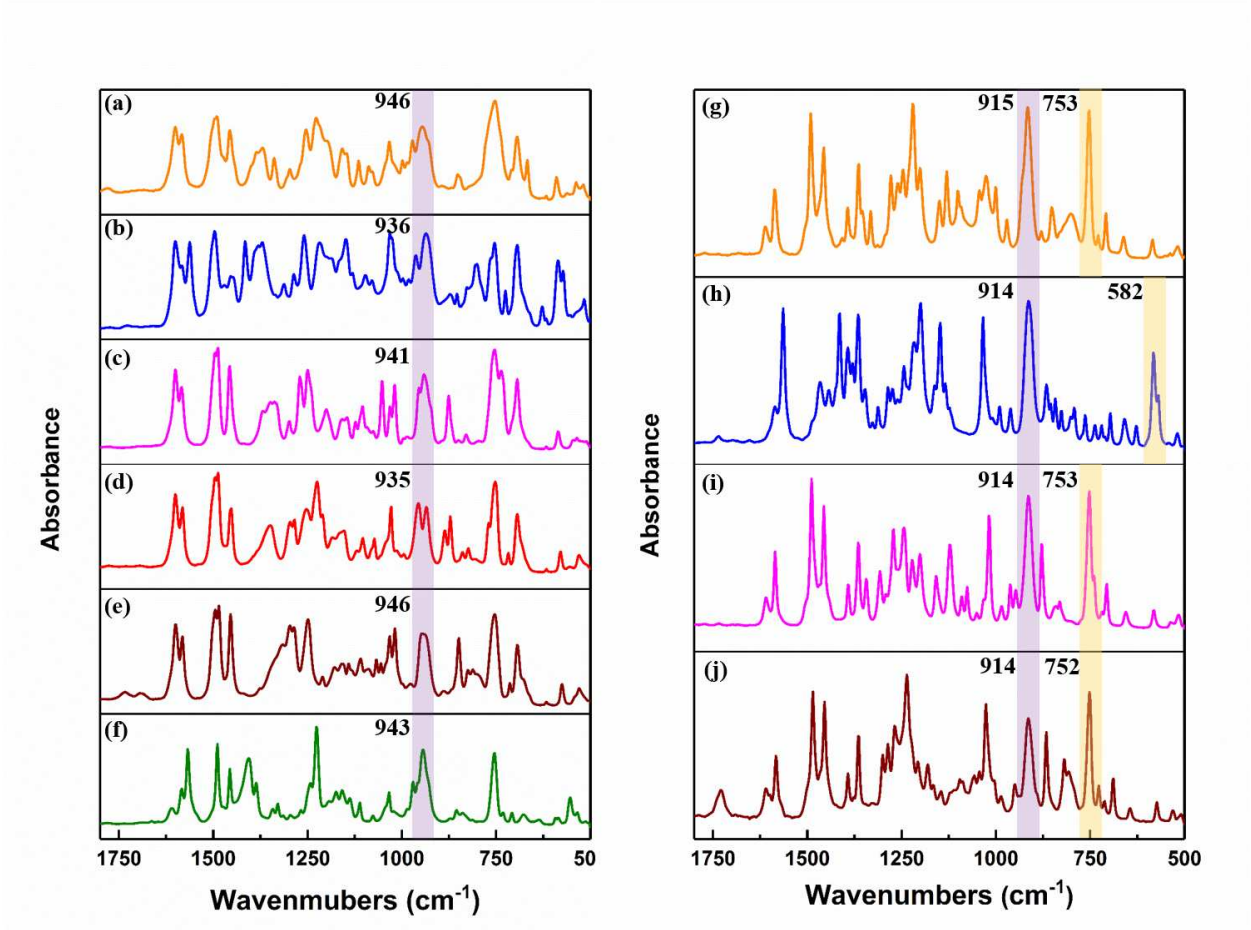

Figure 8. FT-IR spectra of **PH-a** isotopes (left) and **PH-t** isotopes (right). (a) **PH-a**, (b) **PH-a-phenol-d_4**, (c) **PH-a-2oxazine-d_2**, (d) **PH-a-4oxazine-d_2**, (e) **PH-a-oxazine-d_4**, (f) **PH-d-a**, (g) **PH-t**, (h) **PH-t-phenol-d_4**, (i) **PH-t-2oxazine-d_2**, (j) **PH-t-oxazine-d_4**.

3.1.3. ^{15}N-exchanged benzoxazine

Support that this characteristic mode is indeed the oxazine skeletal mode can also be obtained by synthesizing ^{15}N-exchanged monomer, **PH-a-^{15}N**. The synthetic procedure of **PH-a-^{15}N** is shown in Scheme 4.

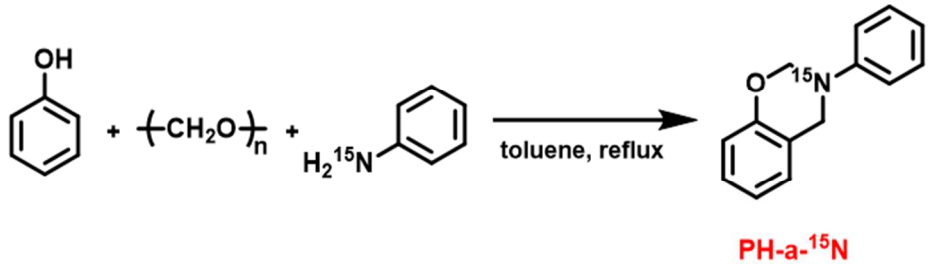

Scheme 4. Synthesis scheme of isotopes of **PH-a-^{15}N**.

The FT-IR spectra of **PH-a** and **PH-a-^{15}N** are shown in Figure 9. The characteristic mode in question for **PH-a** is observed at 946 cm^{-1} whereas that of the ^{15}N isotope exchanged **PH-a** is at 929 cm^{-1}. The shift of the characteristic band from 946 cm^{-1} to 929 cm^{-1} demonstrates that ^{15}N isotope exchange influences the vibration significantly. The band can be either from direct nitrogen atom participation or atoms that are very close to the nitrogen.

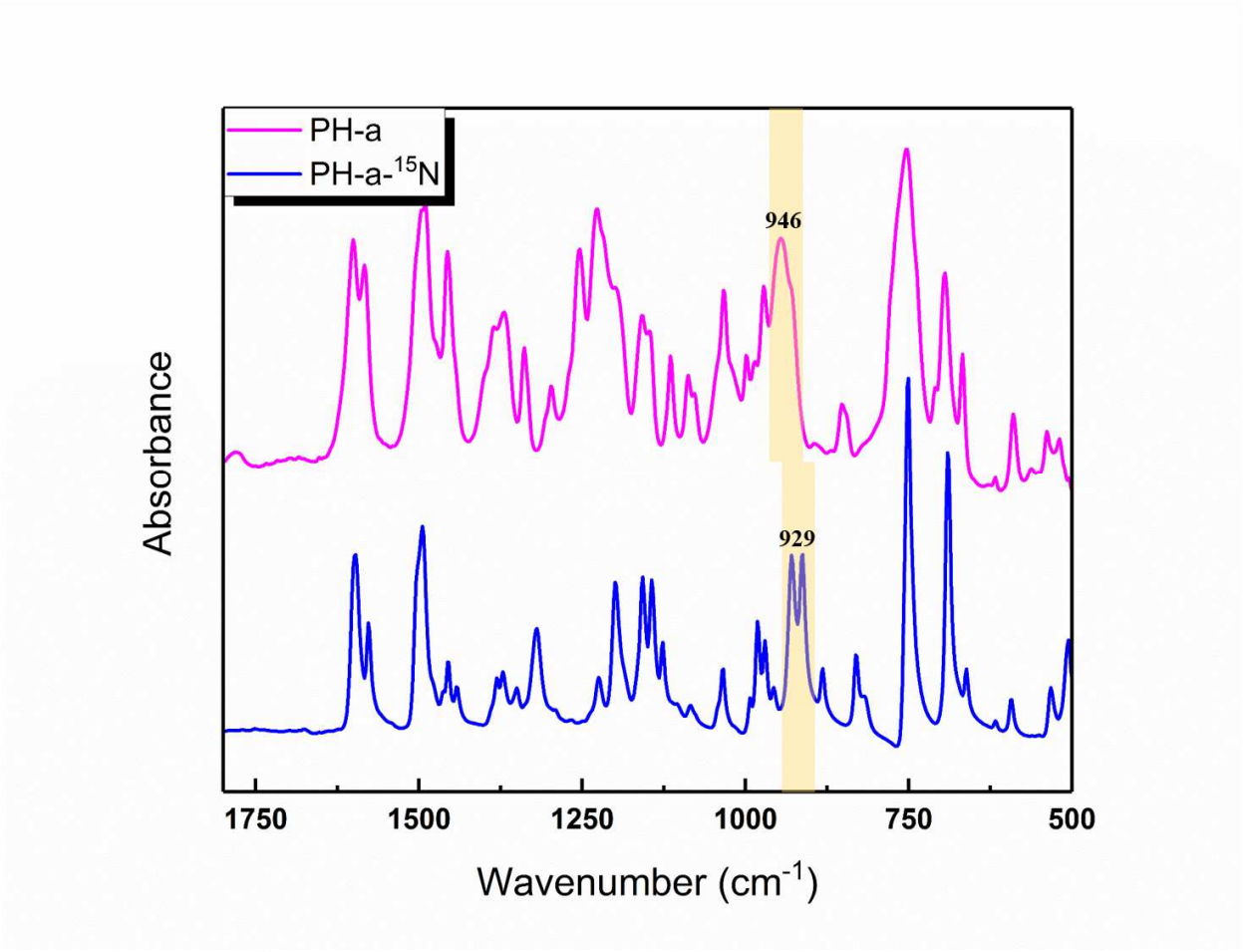

Figure 9. FT-IR spectra of (a) **PH-a**, (b) **PH-a-^{15}N**.

However, at this stage, it is not clear if the vibration is the CN mode related to the O-C-N group or N-C-C group in the oxazine. Therefore, the final compounds synthesized are the oxazine ring with heavier substituent than deuterium at the 2 and 4 positions of the oxazine ring as shown in the synthetic Scheme 5.

3.1.4. Oxazine ring-substituted benzoxazine

Up to now, it has been demonstrated that the characteristic band in question is related to the vibration related to the nitrogen atom and is a skeletal mode. However, it is still not clear

whether the band is from N-C-Ar vibration or O-C-N vibration of the oxazine ring. Two compounds of oxazine ring substituted **PH-a** were used to verify this question.

Two different oxazine ring substituted benzoxazines, **PH-a-4oxazine** and **PH-a-2oxazine**, were obtained as shown in Scheme 5 by multiple step preparation following the **PH-x-2oxazine-d$_2$** synthesis method. The structure of all the compounds were confirmed by ^{1}H-NMR spectra in $CDCl_3$ at room temperature. Both of the compounds show rather high purity. The band for O-CH_2-N split into two doublet resonances due to the difference of the two hydrogen atom in **PH-a-4oxazine**. For **PH-a-2oxazine**, the appearance of two quartet resonance at 4.49-4.55 ppm and 5.62-5.65ppm are attributed to O-*CH*-N and Ar-*CH*$_2$-N, as shown in Figure 10.

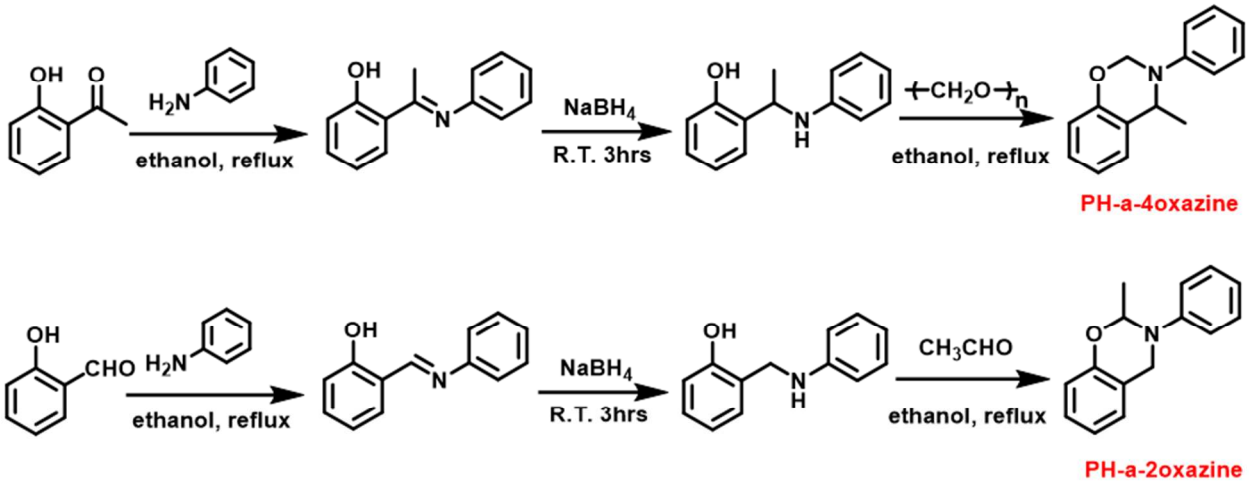

Scheme 5. Synthesis scheme of isotopes of oxazine ring substituted benzoxazine.

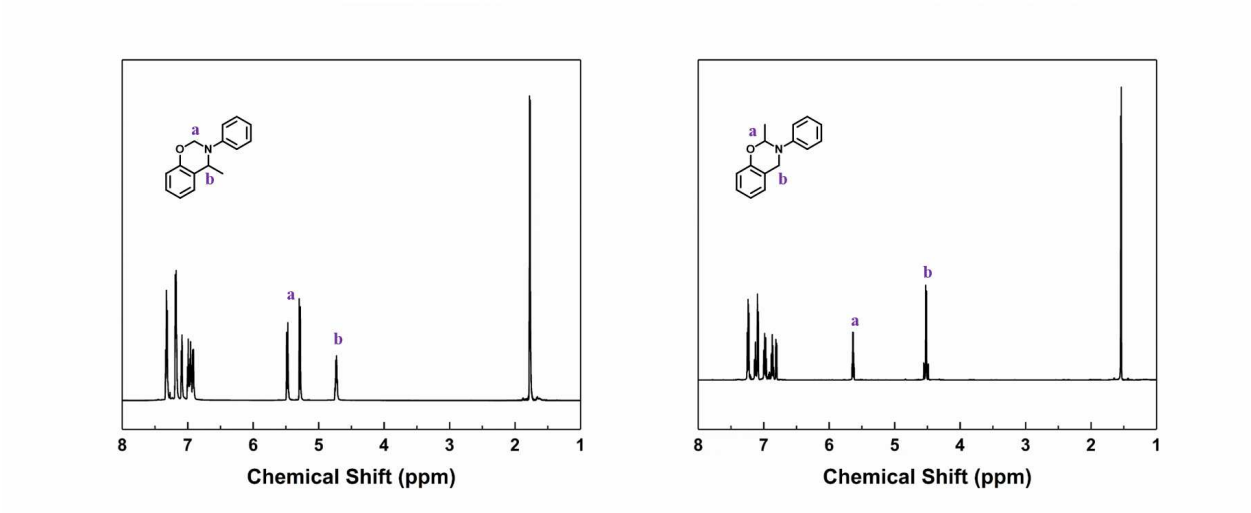

Figure 10. ^{1}H-NMR spectra for **PH-a-4oxazine** and **PH-a-2oxazine** in $CDCl_3$ at room temperature.

Figure 11 shows the comparison of FT-IR spectra of **PH-a-4oxazine** and **PH-a-2oxazine**. Both of them show the characteristic band. When the methyl group substituent is between the nitrogen atom and aromatic ring, the band is at 951cm^{-1} that is + 5 cm^{-1} shift from 946 cm^{-1} of unsabstituted **PH-a**, while the counterpart compound, with the substitution between the oxygen and nitrogen, the characteristic band shifts to 903 cm^{-1} by -43 cm^{-1} and it overlaps with other bands. The frequency shift of this characteristic band is much more significant when the substitution is at the 2-position of the oxazine ring than the 4-position, suggesting that the characteristic band is closely related to O-C-N part compared to C-N-Ar.

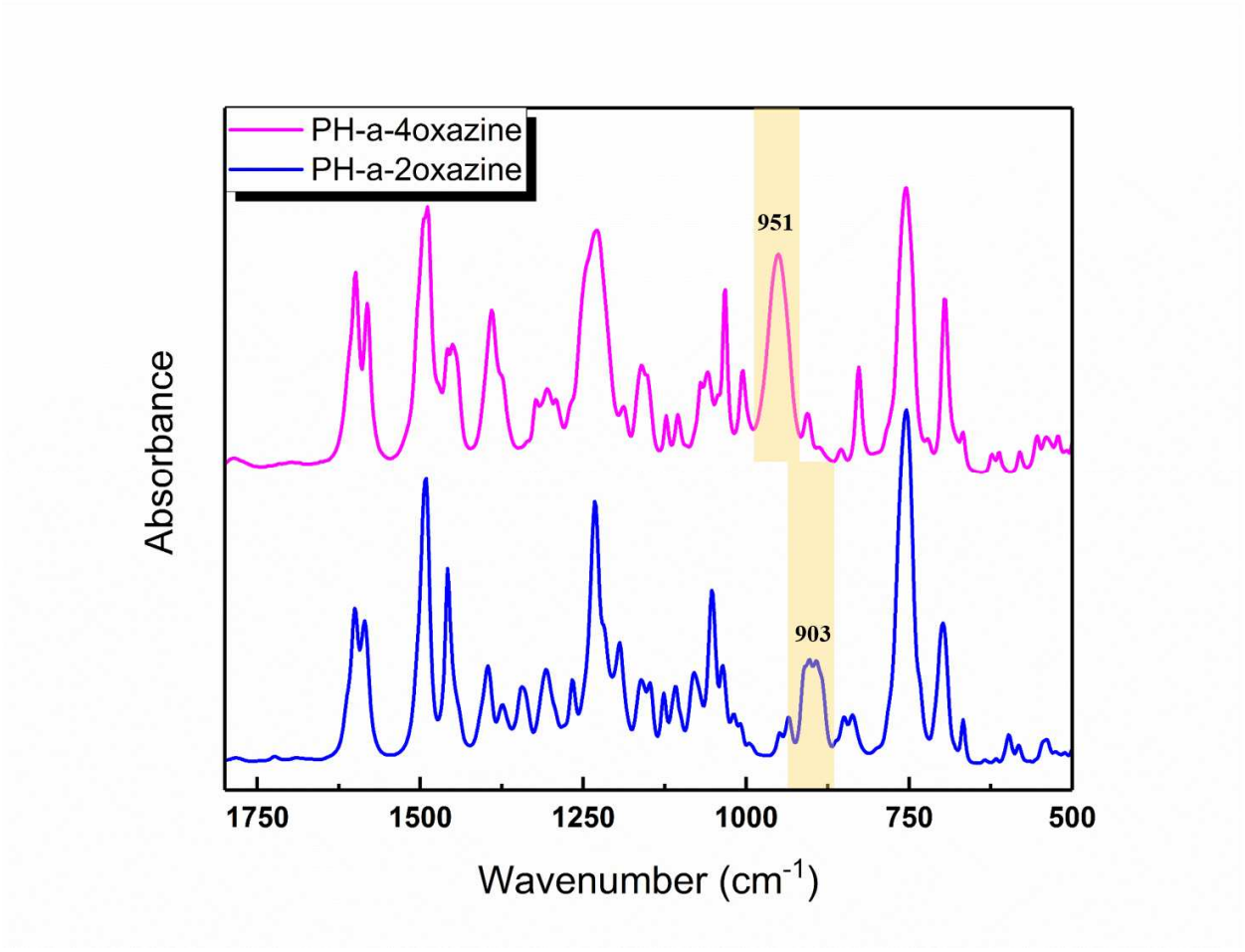

Figure 11. FT-IR spectra of oxazine ring substituted **PH-a**. (a) **PH-a-4oxazine**, (b) **PH-a-2oxazine**.

3.2 Theoretical Calculation

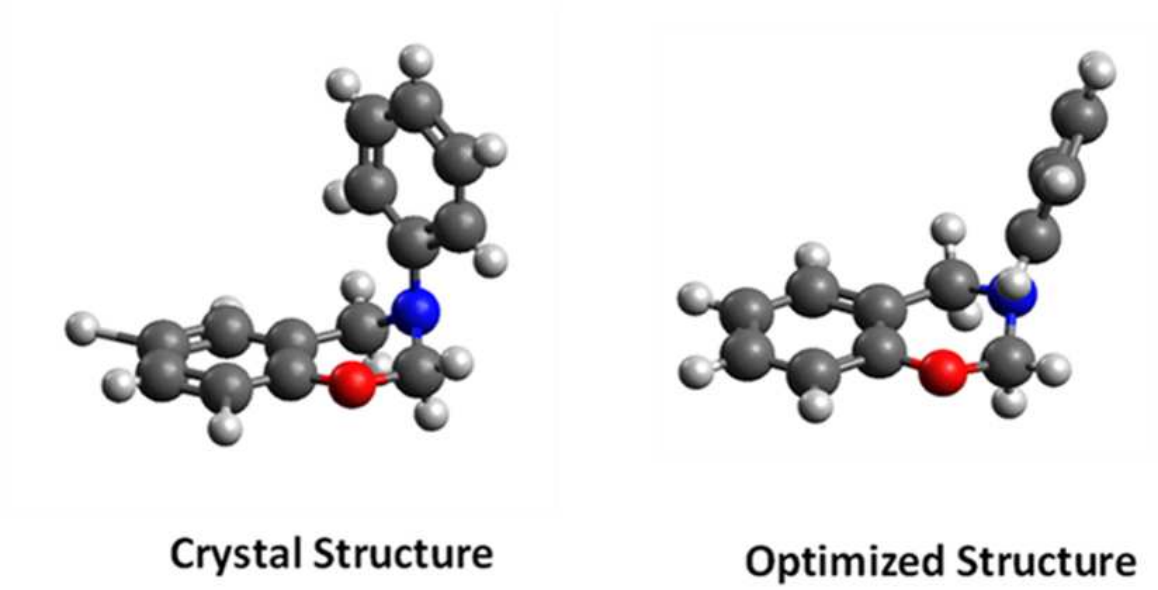

Figure 12. The crystal structure and optimized structure of **PH-a**.

In order to understand the experimental results obtained during the FT-IR analysis of **PH-a** and its isotopes, the corresponding molecules were also studied through a computational point of view. Figure 12 shows the crystal structure and optimized molecular structure of **PH-a**. Compared to the crystalline molecular structure of an analogous compound 3-phenyl-6, 8-dichloro-3, 4-dihydrogen-1, 3-benzoxazine, the aniline ring is rotated ~60°. All other internal coordinates are very similar, all angles were within 5°, and all other torsions are within 15°, showing only slight distortions overall. (See Table S2 in SI).

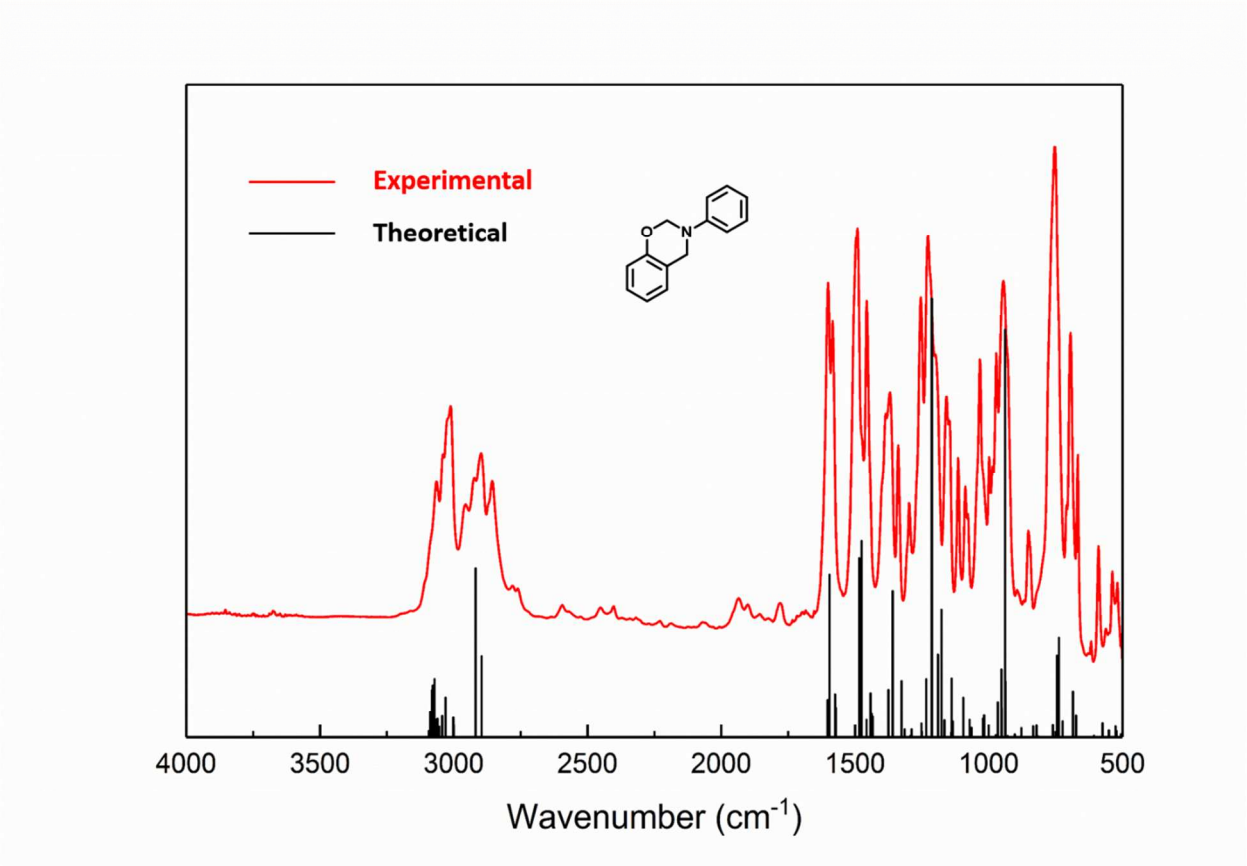

Figure 13. Experimental and theoretical FT-IR results for **PH-a**.

The IR spectra obtained via *ab initio* calculation using the Gaussian program and FT-IR measurement of **PH-a** are shown in Figure 13, showing good agreement between the two after scaling by a factor of 0.970. Since the band assignment of benzoxazine monomer has already been reported and the majority of the band assignment is not controversial, this paper focuses only on the modes heavily related to the oxazine ring. The strong band at 1227 cm^{-1} in the FT-IR spectrum corresponds to the band at 1225 cm^{-1} in the theoretical model. This band has been previously known as the (C-O-C) antisymmetric stretching. The potential energy distribution (PED) shows that the main contributor to this mode is the stretching between the oxygen and the carbon in the phenol ring with a smaller contribution from the torsion of H-C_2-O-C_9. The band that appears overlaid at 1199 cm^{-1} in the experimental FT-IR spectrum, corresponds to the band

at 1188 cm^{-1} in the theoretical model. This band is typically assigned to the (C-N-C) antisymmetric stretching. The PED in this case is given partially by the N-C_2 stretching with smaller contributions from N-C_a and N-C_4.

Lastly, the band at 946 cm^{-1} in the experimental results also appears in the theoretical model at 947 cm^{-1}. Although this band was assigned to the C-H out-of-plane bending of the benzene ring,[18] the experimental results presented in this paper suggests that that is not the only case and it is also proposed to be caused by skeletal O-C_2 stretches. The PED in Table 1 indicates that the main contributor to this mode is the O-C_2 stretching with significant participation of the H-C-C-C torsion (out-of-plain-bending) and C-C-C-C torsion of the phenolic ring and minor contribution of the N-C_2 stretch and H-C_4-C-C torsion.

The complete correlation between the experimental FT-IR and Raman spectra and the theoretical results for **PH-a** and its isotopes are shown in Table S3 in the Supporting Information. All of them show satisfactory agreement as it can be observed in Figure 14, which presents a closer look at the experimental FT-IR and theoretical results for PH-a and isotopes at the fingerprint region.

The corresponding symmetric (C-N-C) stretching can be observed in the Raman spectrum at 737 cm^{-1} as a strong line. The computational model shows the corresponding band at 731 cm^{-1}.

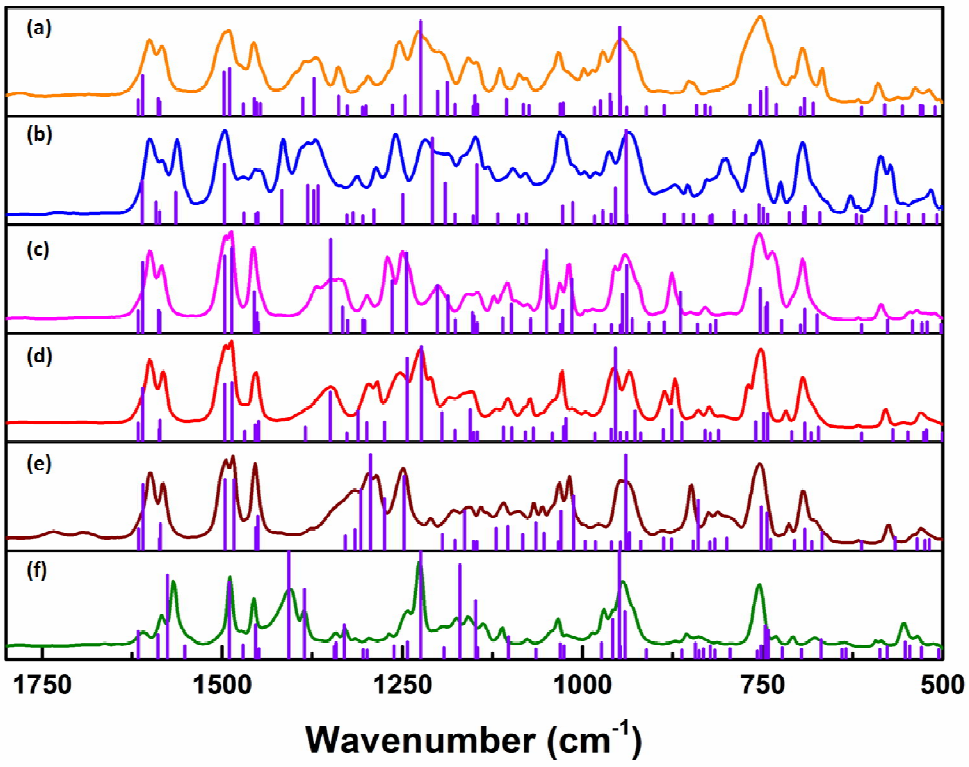

Figure 14. Comparison of experimental FT-IR results and theoretical results for FT-IR spectra of **PH-a** isotopes (a) **PH-a**, (b) **PH-a-phenol-d_4**, (c) **PH-a-2oxazine-d_2**, (d) **PH-a-4oxazine-d_2**, (e) **PH-a-oxazine-d_4**, (f) **PH-d-a**.

Table 1. Potential energy distribution for the oxazine ring-related modes of **PH-a** which is calculated using Gaussian 09 with B3LYP/6-31G** theory and basis and VEDA4 software.

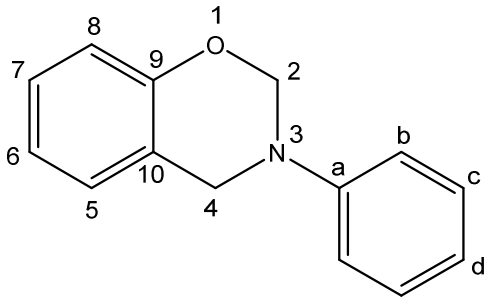

FT-IR (cm^{-1})	Raman (cm^{-1})	Theoretical model (cm^{-1})	Potential energy distribution (%)
2956	2977	2946	C_2-H stretching (92)
2923	2912	2923	C_4-H stretching (95)
	1479	1471	H-C_2-H bend (59)
	1440	1447	H-C_4-H bend (40)
1385	1389	1388	H-C_2-O-C torsion (54)
1370	1367	1373	H-C_2-O-C torsion (19), N-C_a stretch (17), C_2-N-C_4 bend (14)
1339	1341	1339	H-C_4-C-C torsion (30), C-C stretch of phenol ring (28)
1254	1255	1246	H-C_2-O bend (41), H-C_2-O-C torsion (13)
1227	1224	1225	O-C_9 stretch (33), C-C stretch of the phenol ring (14), H-C-C bend of phenol ring (13)
1199	1196	1201	C_9-C_4-H stretch (23), H-C_4-C-C torsion (11)

	1193	1188	C-C-C bend of phenol ring (18), C-C stretch of phenol ring (15), N-C_2 stretch (11)
972	972	975	N-C_4 stretch (25), H-C_2-O-C torsion (14), H-C_2-C-C torsion (12)
		962	N-C_4 stretch (19), N-C_2 stretch (10), O-C_2 stretch (13)
		948	H-C-C-C torsion od phenol ring (63)
946	947	947	O-C_2 stretch (32), H-C-C-C torsion of phenol ring (17)
	737	731	H-C-C bend of phenol ring (39), C-C stretch of phenol ring (13), O-C_9 stretch (10)
		580	H-C-C bend of aniline ring (24), N-C_2-O bend (14), N-C_2 stretch (10)
		556	H-C-C bend of phenol ring (30), C_2-N-C_a bend (11), O-C_9 stretch (8)
	384	362	N-C_2 stretch (20), C_a-N-C_2-O torsion (12), H-C_2-O-C torsion (10)
	323	310	C-C_9-O bend (34), C_a-N-bend (18), H-C-C bend of phenol ring (9)
	293	286	C-C-C-C torsion of phenol ring (35), C_2-O-C-C torsion (12)

Table 2. Frequency of the characteristic band in experimental FT-IR and Raman and theoretical model for **PH-a**, **PH-a-phenol-d_4**, **PH-a-2oxazine-d_2**, **PH-a-4oxazine-d_2**, **PH-a-oxazine-d_4**, **PH-d-a** and **PH-a-^{15}N**.

PH-a isotopes	FT-IR (cm^{-1})	Raman (cm^{-1})	Theoretical model (cm^{-1})
PH-a	946	947	947
PH-a-phenol-d_4	936	934	939
PH-a-2oxazine-d_2	941	949	945
PH-a-4oxazine-d_2	956	962	954
PH-a-oxazine-d_4	946	944	940
PH-d-a	943	961	951
PH-a-^{15}N	929	932	946

The comparison between the experimental FT-IR and Raman results and the predicted value for the characteristic band are presented in Table 2. All the results show that the theoretical model accurately predicts the trend in the direction of frequency shift of the characteristic band with small differences in the magnitude. It is also clear that this particular mode is not a pure one, which is why the isotopic substitution in the phenol portion of the benzoxazine or the oxazine portion both causes an impact in the frequency of the characteristic band. This is also substantiated by the potential energy distribution of **PH-a** (Table S4). PED indicates that 48% of this mode is caused by different vibrations in the oxazine ring and 30% is caused by the phenol portion of the molecule, which is why the selective deuteration of different parts of **PH-a** presents a shifting in this particular mode. This heavily mixed mode is in part the reason why previously this mode was assigned to the C-H mode of benzene to which oxazine is attached. However, this mode completely disappears rather than shift its position upon ring opening of the

oxazine group.[7,18] Thus, it is more appropriate to assign this mode to the oxazine group related and, more specifically, to O-C-N group rather than N-C-C group of the oxazine as the N-C-C group still exists even in the ring opened compound.

3.3 Deconvolution of Vibrational Bands

The previous discussion reveals that the characteristic band is not a pure band in the following three aspects: (1) In the experimental results, the characteristic band always appears regardless of the position of the deuterium substitution; (2) In the theoretical calculation, three main vibrational modes contribute to the characteristic band in the Potential Energy Distribution (3) By visual inspection, the band clearly does not conform to a single Gaussian-Lorentz contour and, indeed, even a shoulder can be observed which then disappears upon polymerization of the monomer.

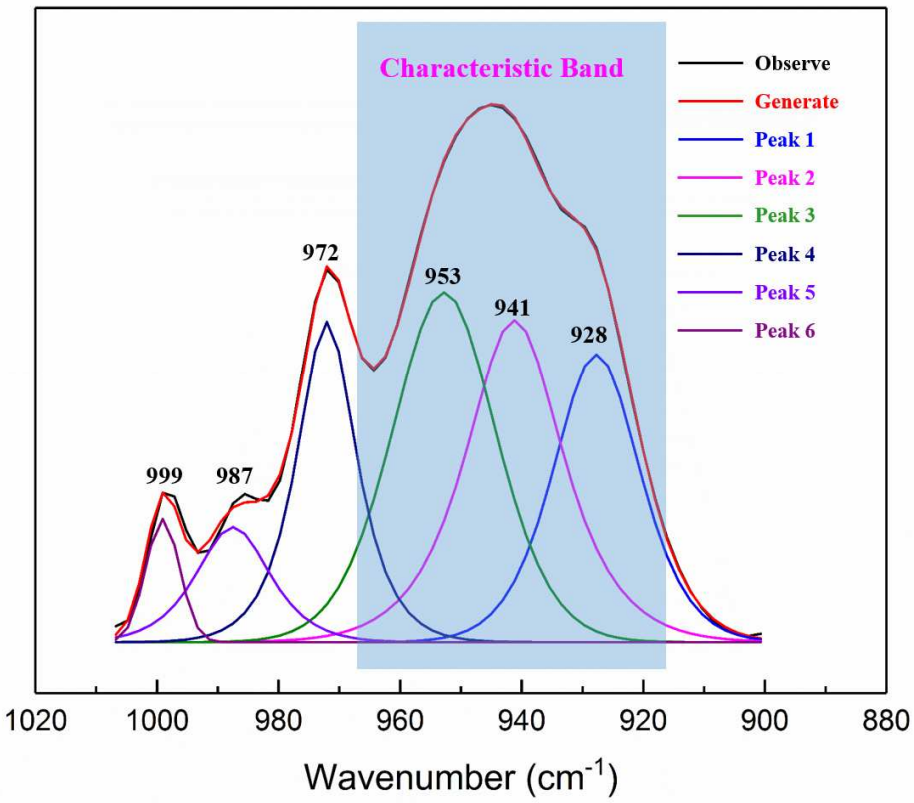

Figure 15. Characteristic band fitting of FT-IR spectrum of **PH-a**.

Figure 15 shows an example deconvolution of this characteristic band can be fit into three Gaussian* Lorenz bands. The peak position of these three bands are 953, 941 and 928 cm^{-1}. The three bands can be corresponded to 948, 947 and 939 cm^{-1} in the theoretical calculation. Therefore, H-C-C-C torsion of phenol ring (948), O-C_2 stretch and H-C-C-C torsion of phenol ring (947), and H-C-C-C torsion of aniline ring (939) all contribute to the characteristic band. It is thus safe to conclude this band is not a pure band.

3.4 Band Assignment

Comparing the region between 3200 cm^{-1} and 2800 cm^{-1} in FT-IR spectra, which represents the C-H stretching in aromatic (greater than 3000 cm^{-1}) and in aliphatic (3000 cm^{-1} to 2800 cm^{-1}) part, the band positions are almost the same.

In the range of 2800cm-1 to 1600cm^{-1}, the C-D stretching vibration is very obvious from the comparison of the **PH-a** series FT-IR spectra (Figure 8, left and Figure 9). Expectedly, **PH-a** does not show any band in the range of 3000cm-1 to 2000cm^{-1}. **PH-a-phenol-d_4** shows the C-D stretching band at 2278 cm^{-1}, which corresponds to the aromatic C-D stretching. **PH-a-2oxazine-d_2** shows the C-D stretching band at 2150 cm^{-1}, **PH-a-4oxazine-d_2** at 2121 cm^{-1}, and **PH-a-oxazine-d_4** at 2146 cm^{-1}, and **PH-d-a** at 2275 cm^{-1}. The three isotopes of oxazine deuteration at 2, 4 positions and both, shows smaller wavenumbers compared to the aromatic deuteration. It shows the same behavior of the corresponding C-H stretching.

In Table S3, the region between 1600 cm^{-1} to 1440 cm^{-1} is the aromatic skeletal mode. Four main modes are shown in this region. 1601(s), 1584(s), 1491(vs), 1456(s) in the FT-IR spectrum and 1602 (m), 1583(w), 1492(vw), 1453(m) cm^{-1} in the Raman spectrum. Comparing these regions, the most obvious difference comes from **PH-a-phenol-d_4**, a very strong band appears at 1562 cm^{-1}, which might come from the deuteration of the benzene ring on the phenol part. The other difference comes from the **PH-a-^{15}N**. **PH-a-^{15}N** shows one less strong band at the positon of around 1455cm^{-1}, instead, it becomes a weak band. It is probably due to the isotope ^{15}N influence on the skeletal mode.

In the range from 1440 cm^{-1} to 1210 cm^{-1}, the range represents the CH_2 vibration of the oxazine ring. The relatively strong band in the FT-IR spectra from 1227 cm^{-1} to 1218 cm^{-1} is the asymmetric C-O-C vibration. For **PH-a**, **PH-a-phenol-d_4**, **PH-a-4oxazine-d_2** and **PH-d-a** the

isotopes do not influence the asymmetric C-O-C vibration, therefore, the bands appears at 1227, 1218, 1225, 1226 cm^{-1} with a shoulder on the right side of the bands, respectively. On the other hand, the bands of asymmetric C-O-C vibration will be significantly influenced due to the substitution on 2 positon, both 2 and 4 position isotope of **PH-a-2oxazine-d_2** and **PH-a-oxazine-d_4**. Therefore, the band for these three isotope compounds disappeared in this region and shifts to lower wavenumbers, from 1210 cm^{-1} to 1200 cm^{-1}, respectively. One skeletal vibration appears at 1158, 1149, 1146, 1154, 1157, 1158 and 1159 cm^{-1} for **PH-a**, **PH-a-phenol-d_4**, **PH-a-2oxazine-d_2**, **PH-a-4oxazine-d_2**, **PH-a-oxazine-d_4**, **PH-a-^{15}N** and **PH-d-a** respectively. The skeletal vibration is influenced by the isotope substitution on benzene ring and oxazine ring. Therefore, without isotope substitution on benzene ring and oxazine ring, **PH-a** and **PH-a-^{15}N** show the original band at 1158 cm^{-1}. The band shifts to lower wavenumbers with the deuteration. For symmetric C-O-C vibration, the shift based on the isotope position is quite obvious. The band appears at 1033, 1031, 1029, 1034, 1034 cm^{-1} for **PH-a**, **PH-a-phenol-d_4**, **PH-a-4oxazine-d_2**, **PH-a-^{15}N** and **PH-d-a** when no isotope substitution near oxygen atom. The band for **PH-a-2oxazine-d_2** and **PH-a-oxazine-d_4** shift to 1019 cm^{-1} and 1018 cm^{-1}.

In the range of characteristic band, broad bands appear for all the **PH-a** isotopes. Incidentally, the C-H out-of-plane bending and O-C_2-N stretching overlaps. **PH-a**, broad band at 946 cm^{-1}, shoulder on right, **PH-a-phenol-d_4**, broad band at 936 cm^{-1}, shoulder on right, **PH-a-4oxazine-d_2** shows a sharp band at 935 cm^{-1} , **PH-a-2oxazine-d_2** shows a broad band at 941 cm^{-1}, **PH-a-oxazine-d_4** shows a broad band at 946 cm^{-1}, **PH-a-^{15}N** is at 929 cm^{-1} a sharp band, PH-d-a shows a broad band at 943 cm^{-1}. The band position was not influenced significantly by the isotopes since the deuterium does not participate in the stretching vibration. Integrated band assignment information can be found in Table S3 in SI.

4. CONCLUSION

All substituted benzoxazines, **PH-a** and **PH-t** isotope series, and oxazine ring substituted benzoxazine were successfully synthesized and the structures were confirmed by ^{1}H NMR. FT-IR results of all substituted benzoxazine results show that the previously assigned characteristic band for benzoxazine at 960-900 cm^{-1} is not only related to C-H out-of-plane bending, but also oxazine skeletal vibrations significantly contribute to this band. ^{15}N isotope compound further demonstrated the band is related to a vibration in which the oxazine ring is involved. C_2 and C_4 substituted oxazine ring benzoxazine results show that, when the substitution is between the oxygen and nitrogen atoms, the characteristic band is influenced the most. The results of the theoretical calculation are consistent with the experimental results. The deconvolution of the characteristic FT-IR band in question shows that this band is not a pure band, instead, it is a contribution of three main vibrations. Therefore, we conclude the characteristic band near 930 cm^{-1} is mainly related to the oxazine ring, the vibration of O-C_2 vibration with a minor contribution from the phenolic ring.

5. SUPPORTING INFORMATION

NMR spectra (Figure S1.- Figure S15.), FTIR Spectra (Figure S16.- Figure S31), Raman Spectra (Figure S32.- Figure 42.) and theoretical calculation (Figure S43.- Figure 49.) of all the compounds used for the study, determination of scaling factor (Table S1.), comparison between crystal and Gaussian optimized structure for PH-a (Table S2.), band assignment (Table S3.) and Potential energy distribution of PH-a (Table S4.)

6. ACKNOWLEDGMENT

One of the authors (D.I.) gratefully acknowledge the partial support of SBIR Phase II grant No. NNX15CL03C from the National Aeronautical and Space Administration (NASA) under the subcontract from Materials Answers LLC. V.S. also acknowledge the financial support for the summer REU program from the National Science Foundation (NSF) under the grant No. DMR 0423914. The authors are also indebted to the generous permission for the use of supercomputer at the Ohio State University Supercomputer facility.

REFERENCES

(1) Ishida, H.; Allen, D. J. Physical and Mechanical Characterization of Near-zero Shrinkage Polybenzoxazines. *J. Polym. Sci. Part B: Polym. Phys.* **1996**, *34*, 1019-1030.

(2) Ishida, H.; Allen, D. J. Gelation Behavior of Near-zero Shrinkage Polybenzoxazines. *J. Appl. Polym. Sci.* **2001**, *79*, 406-417.

(3) Low, H. Y.; Ishida, H. Mechanistic Study on the Thermal Decomposition of Polybenzoxazines: Effects of Aliphatic Amines. *J. Polym. Sci. Part B: Polym. Phys.* **1998**, *36*, 1935-1946.

(4) Wang, C.-F.; Su, Y.-C.; Kuo, S.-W.; Huang, C.-F.; Sheen, Y.-C.; Chang, F.-C. Low-Surface-Free-Energy Materials Based on Polybenzoxazines. *Angew. Chem., Int. Ed.* **2006**, *45*, 2248-2251.

(5) Liu, J.; Lu, X.; Xin, Z.; Zhou, C. Synthesis and Surface Properties of Low Surface Free Energy Silane-Functional Polybenzoxazine Films. *Langmuir* **2013**, *29*, 411-416.

(6) Chernykh, A.; Agag, T.; Ishida, H. Synthesis of Linear Polymers Containing Benzoxazine Moieties in the Main Chain with High Molecular Design Versatility via Click Reaction. *Polymer* **2009**, *50*, 382-390.

(7) Agag, T.; Takeichi, T. Novel Benzoxazine Monomers Containing *p*-Phenyl Propargyl Ether: Polymerization of Monomers and Properties of Polybenzoxazines. *Macromolecules* **2001**, *34*, 7257-7263.

(8) Han, L.; Zhang, K.; Ishida, H.; Froimowicz, P. Study of the Effects of Intramolecular and Intermolecular Hydrogen-Bonding Systems on the Polymerization of Amide-Containing Benzoxazines. *Macromol. Chem. Phys.* **2017**, in press, DOI: 10.1002/macp.201600562.

(9) Sawaryn, C.; Landfester, K.; Taden, A. Benzoxazine Miniemulsions Stabilized with Polymerizable Nonionic Benzoxazine Surfactants. *Macromolecules* **2010**, *43*, 8933-8941.

(10) Li, X.; Gu, Y. The Co-curing Process of a Benzoxazine-cyanate System and the Thermal Properties of the Copolymers. *Polym. Chem.* **2011**, *2*, 2778-2781.

(11) Alhwaige, A. A.; Agag, T.; Ishida, H.; Qutubuddin, S. Biobased Chitosan/Polybenzoxazine Cross-Linked Films: Preparation in Aqueous Media and Synergistic Improvements in Thermal and Mechanical Properties. *Biomacromolecules* **2013**, *14*, 1806-1815.

(12) Froimowicz, P.; R. Arza, C.; Han, L.; Ishida, H. Smart, Sustainable, and Ecofriendly Chemical Design of Fully Bio-Based Thermally Stable Thermosets Based on Benzoxazine Chemistry. *ChemSusChem* **2016**, *9*, 1921-1928.

(13) Ning, X.; Ishida, H. Phenolic Materials via Ring-opening Polymerization of Benzoxazines: Effect of Molecular Structure on Mechanical and Dynamic Mechanical Properties. *J. Polym. Sci. Part B: Polym. Phys.* **1994**, *32*, 921-927.

(14) Allen, D. J.; Ishida, H. Physical and Mechanical Properties of Flexible Polybenzoxazine Resins: Effect of Aliphatic Diamine Chain Length. *J. Appl. Polym. Sci.* **2006,** *101*, 2798-2890.

(15) Ishida, H.; Allen, D. J. Mechanical Characterization of Copolymers Based on Benzoxazine and Epoxy. *Polymer* **1996**, *37*, 4487-4495.

(16) Kiskan, B.; Yagci, Y.; Ishida, H. Synthesis, Characterization, and Properties of New Thermally Curable Polyetheresters Containing Benzoxazine Moieties in the Main Chain. *J. Polym. Sci.Part A: Polym. Chem.* **2008**, *46*, 414-420.

(17) Santhosh Kumar, K. S.; Reghunadhan Nair, C. P.; Sadhana, R.; Ninan, K. N. Benzoxazine–bismaleimide Blends: Curing and Thermal Properties. *Eur. Polym. J.* **2007**, *43*, 5084-5096.

(18) Dogan Demir, K.; Kiskan, B.; Yagci, Y. Thermally Curable Acetylene-Containing Main-Chain Benzoxazine Polymers via Sonogashira Coupling Reaction. *Macromolecules* **2011**, *44*, 1801-1807.

(19) Dunkers, J.; Ishida, H. Vibrational Assignments of 3-alkyl-3,4-dihydro-6-methyl-2H-1,3-benzoxazines in the Fingerprint Region. *Spectrochim. Acta. A-M.* **1995**, *51*, 1061-1074.

(20) Dunkers, J.; Zerate, E.A.; Ishida, H. Crystal Structure and Hydrogen-Bonding Characteristics of *N,N*-Bis(3,5-dimethyl-2-hydroxybenzyl)methylamine, A Benzoxazine Dimer. *J. Phys. Chem.* **1996**, *100*, 13514-13520.

(21) Ning, X.; Ishida, H. Phenolic Materials via Ring-opening Polymerization: Synthesis and Characterization of Bisphenol-A Based Benzoxazines and Their Polymers. *J. Polym. Sci. Part A: Polym. Chem.* **1994**, *32*, 1121-1129.

(22) Ohashi, S.; Pandey, V.; Arza, C. R.; Froimowicz, P.; Ishida, H. Simple and Low Energy Consuming Synthesis of Cyanate Ester Functional Naphthoxazines and Their Properties. *Polym. Chem.* **2016**, *7*, 2245-2252.

(23) Andreu, R.; Ronda, J. C. Synthesis of 3,4-Dihydro-2H-1,3-benzoxazines by Condensation of 2-Hydroxyaldehydes and Primary Amines: Application to the Synthesis of Hydroxy-Substituted and Deuterium-Labeled Compounds. *Synthetic Commun.* **2008**, *38*, 2316-2329.

(24) Rudyanto, M.; Ekowati, J.; Widiandani, T.; Honda, T. Synthesis and Brine Shrimp Lethality Test of Some Benzoxazine and Aminomethyl Derivatives of Eugenol. *Int. J. Pharm. Pharm. Sci.* **2014**, *6*, 465-467.

(25) Keresztury, G.; Holly, S.; Besenyei, G.; Varga, J.; Wang, A.; Durig, J. R. Vibrational Spectra of Monothiocarbamates-II. IR and Raman Spectra, Vibrational Assignment, Conformational Analysis and ab initio Calculations of S-methyl-*N,N*-dimethylthiocarbamate. *Spectrochim. Acta A-M.* **1993**, *49*, 2007-2017.

(26) Mohan, S.; Sundaraganesan, N.; Mink, J. FTIR and Raman Studies on Benzimidazole. *Spectrochim. Acta. A-M.* **1991**, *47*, 1111-1115.

(27) Wang, M-W.; Jeng, R-J.; Lin, C-H. Study on the Ring-Opening Polymerization of Benzoxazine through Multisubstituted Polybenzoxazine Precursors. *Macromolecules* **2015**, *48*, 530-535.

(28) Kohn, W.; Sham, L. J. Self-Consistent Equations Including Exchange and Correlation Effects. *Phys. Rev.* **1965**, *140*, A1133-A1138.

(29) Pople, J. A.; Gill, P. M. W.; Johnson, B. G. Kohn—Sham Density-Functional Theory within a Finite Basis Set. *Chem. Phys. Lett.* **1992**, *199*, 557-560.

(30) Becke, A. D. Density‐functional Thermochemistry. III. The role of Exact Exchange. *J. Chem. Phys.* **1993**, *98*, 5648-5652.

(31) Lee, C.; Yang, W.; Parr, R. G. Development of the Colle-Salvetti correlation-energy formula into a functional of the electron density. *Phys. Rev. B* **1988**, *37*, 785-789.

(32) Vosko, S. H.; Wilk, L.; Nusair, M. Accurate Spin-dependent Electron Liquid Correlation Energies for Local Spin Density Calculations: a Critical Analysis. *Can. J. Phys.* **1980**, *58*, 1200-1211.

(33) Stephens, P. J.; Devlin, F. J.; Chabalowski, C. F.; Frisch, M. J. Ab Initio Calculation of Vibrational Absorption and Circular Dichroism Spectra Using Density Functional Force Fields. *J. Phys. Chem.* **1994**, 98, 11623-11627.

(34) Hehre, W. J.; Ditchfield, R.; Pople, J. A. Self—Consistent Molecular Orbital Methods. XII. Further Extensions of Gaussian—Type Basis Sets for Use in Molecular Orbital Studies of Organic Molecules. *J. Chem. Phys.* **1972**, *56*, 2257-2261.

(35) Krishnan, R.; Binkley, J. S.; Seeger, R.; Pople, J. A. Self - consistent Molecular Orbital Methods. XX. A Basis Set for Correlated Wave Functions. *J. Chem. Phys.* **1980**, *72*, 650-654.

(36) Liu, X.; Gu, Y. Effects of Molecular Structure Parameters on Ring-opening Reaction of Benzoxazines. *Sci. China Ser. B* **2001**, *44*, 552-560.

(37) Bartell, L. S.; Roth, E. A.; Hollowell, C. D.; Kuchitsu, K.; Jr., J. E. Y. Electron - Diffraction Study of the Structures of C_2H_4 and C_2D_4. *J. Chem. Phys.* **1965**, *42*, 2683-2686.

(38) Hanwell, M. D.; Curtis, D. E.; Lonie, D. C.; Vandermeersch, T.; Zurek, E.; Hutchison, G. R. Avogadro: an Advanced Semantic Chemical Editor, Visualization, and Analysis Platform. *J. Cheminformatics* **2012**, 4:17.

(39) Frisch, M. J.; Trucks, G. W.; Schlegel, H. B.; Scuseria, G. E.; Robb, M. A.; Cheeseman, J. R.; Scalmani, G.; Barone, V.; Mennucci, B.; Petersson, G. A., et al. *Gaussian 09*, Revision A.1; Gaussian, Inc.: Wallingford, CT, 2009.

(40) Hehre, W. J. Lathan, W.A.; Ditchfield, R.; Newton, M.D.; Pople, J.A. *Gaussian 70* (Quantum Chemistry Program Exchange, Program **1970**, No. 237.

(41) O'Boyle, N. M.; Tenderholt, A. L.; Langner, K. M. cclib: A Library for Package-Independent Computational Chemistry Algorithms. *J. Comput. Chem.* **2008**, *29*, 839-845.

(42) Irikura, K. K.; Johnson III, R. D.; Kacker, R. N. Uncertainties in Scaling Factors for ab initio Vibrational Frequencies. *J. Phys. Chem. A.* **2005**, *109*, 8430-8437.

(43) Jamróz, M. H. Vibrational Energy Distribution Analysis (VEDA): Scopes and Limitations. *Spectrochim. Acta. A-M*. **2013**, *114*, 220-230.

(44) Heyes, C. D.; El-Sayed, M. A. Effect of Temperature, pH, and Metal Ion Binding on the Secondary Structure of Bacteriorhodopsin: FT-IR Study of the Melting and Premelting Transition Temperatures. *Biochemistry* **2001**, *40*, 11819-11827.

(45) Nguyen-Thai, N. U.; Hong, S. C. Structural Evolution of Poly(acrylonitrile-co-itaconic acid) during Thermal Oxidative Stabilization for Carbon Materials. *Macromolecules* **2013**, *46*, 5882-5889.

TOC Graphic

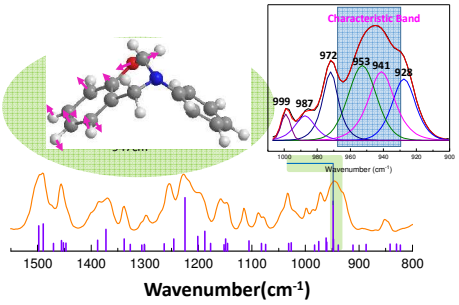
Characteristic Band
999
987
972
953
941
928
1500
1400
1300
1200
1100
1000
900
800
Wavenumber(cm-1)

223x72mm (150 x 150 DPI)

163x112mm (150 x 150 DPI)

176x47mm (150 x 150 DPI)

96x49mm (150 x 150 DPI)

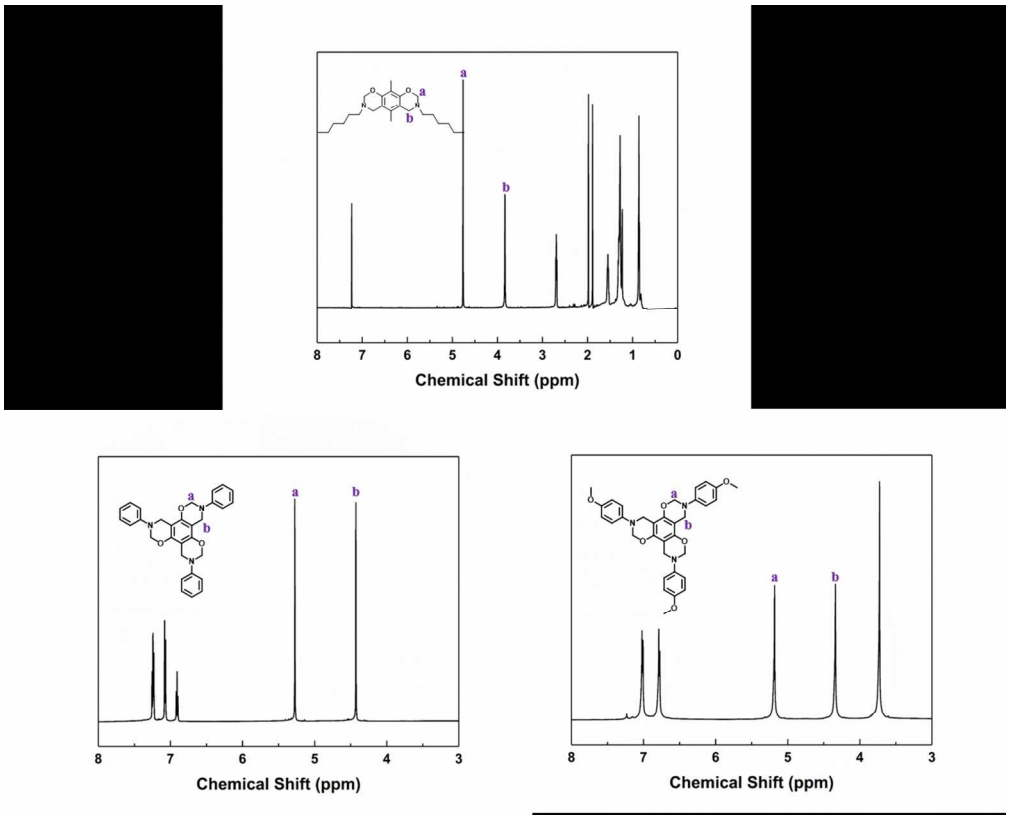

220x177mm (150 x 150 DPI)

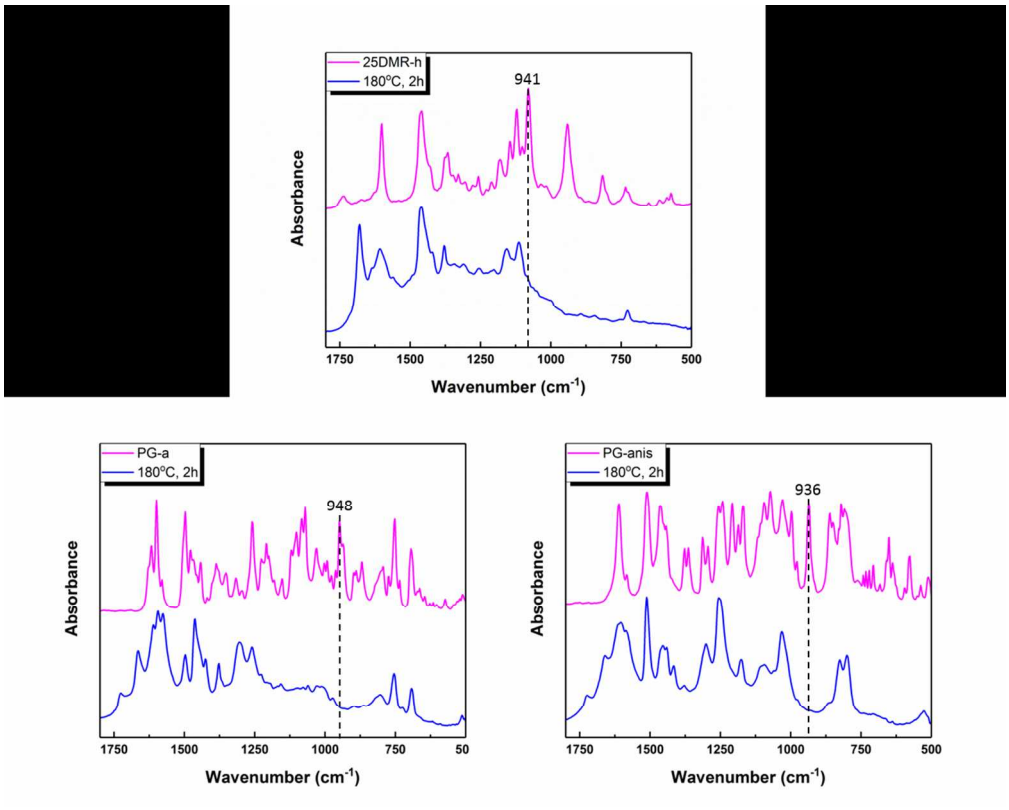

217x173mm (150 x 150 DPI)

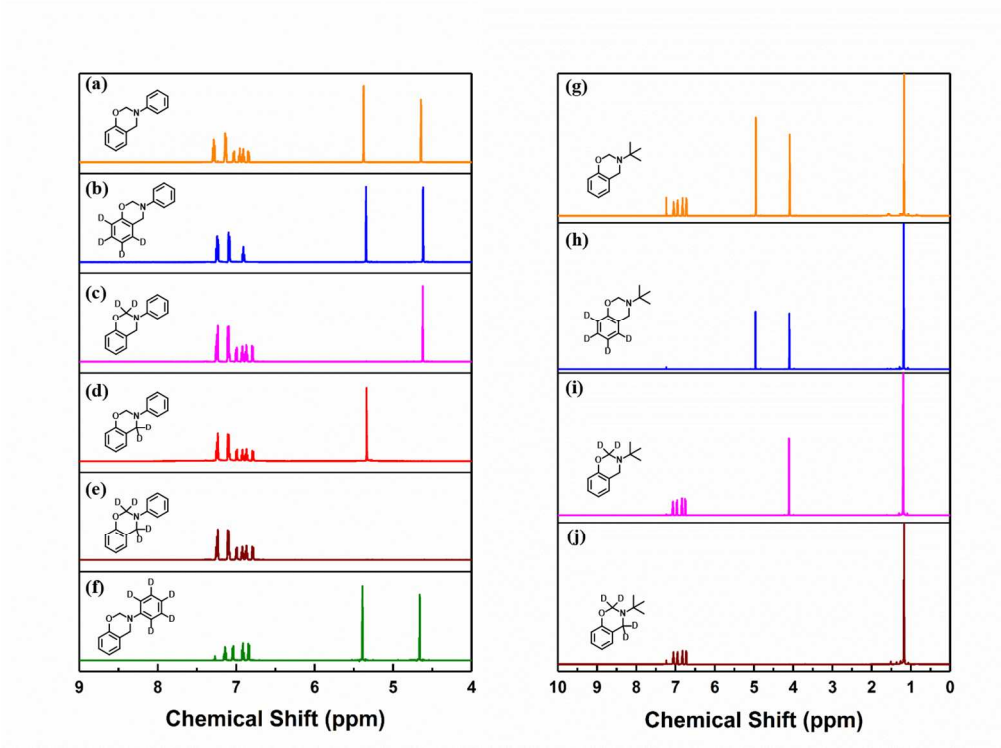

254x190mm (150 x 150 DPI)

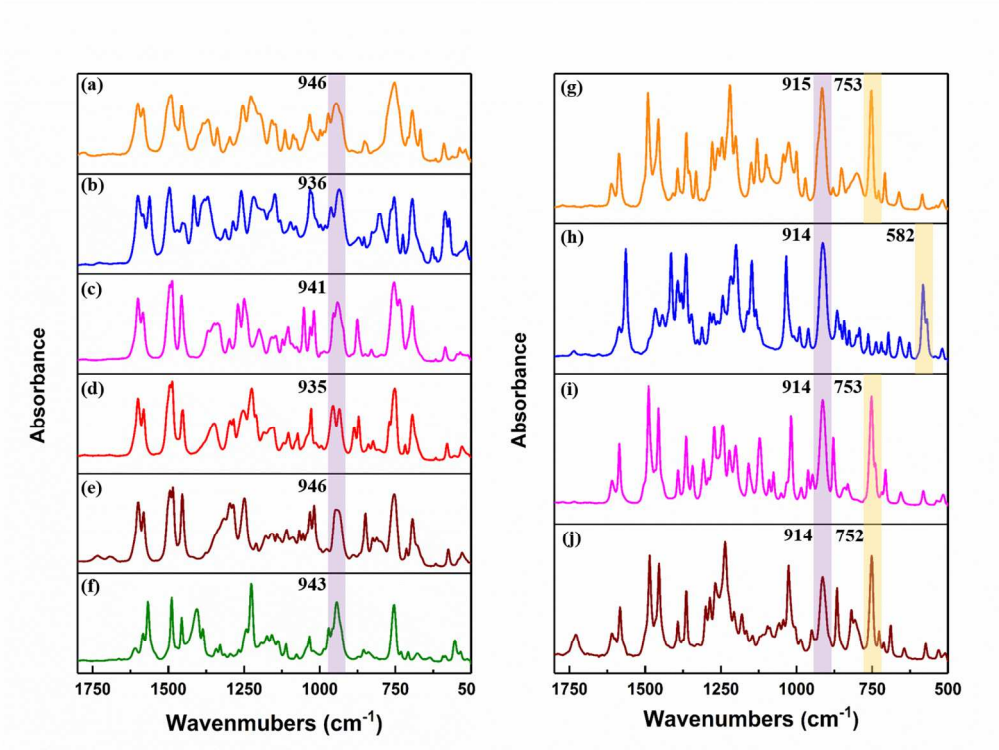

254x190mm (150 x 150 DPI)

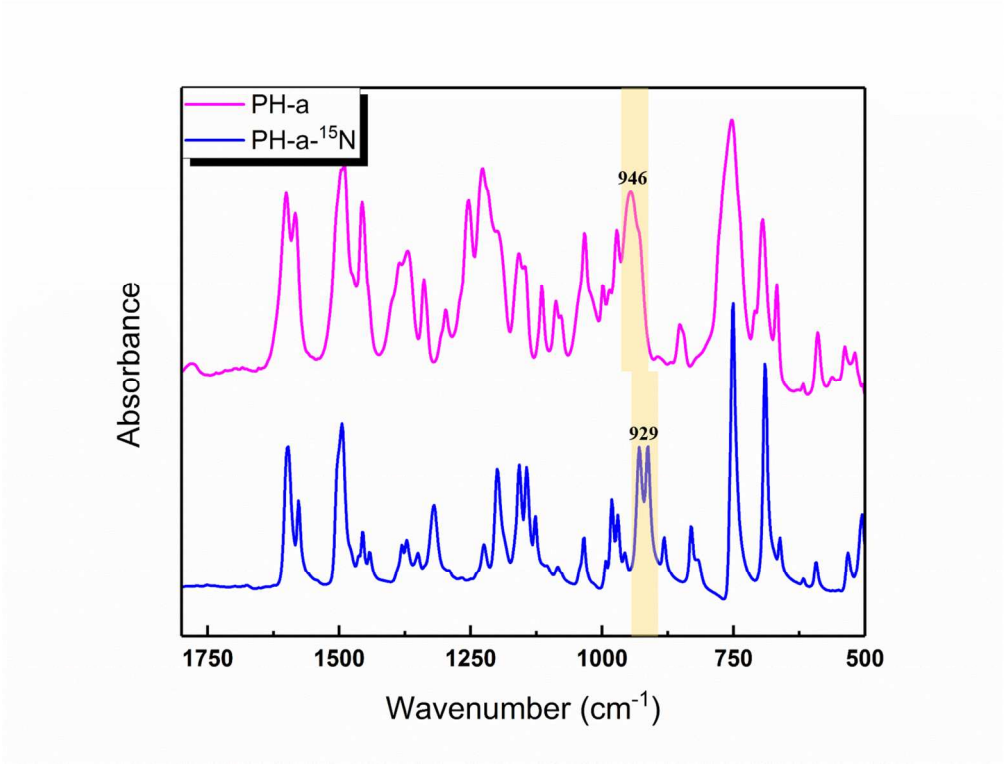

248x190mm (150 x 150 DPI)

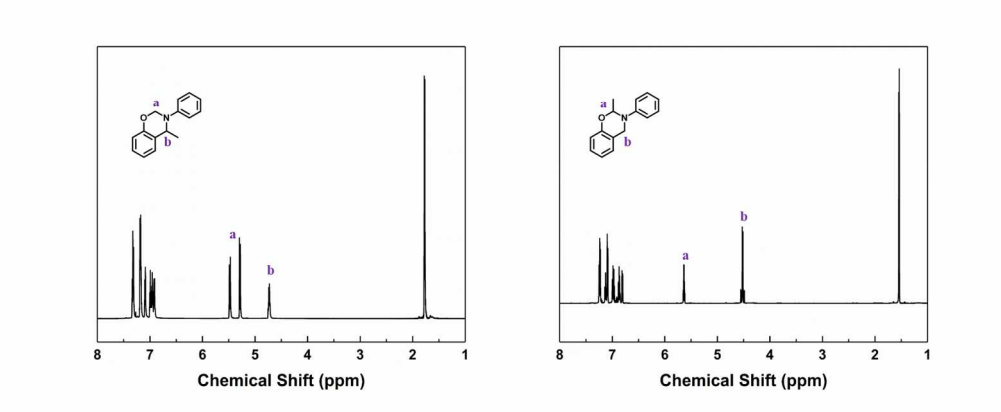

308x127mm (150 x 150 DPI)

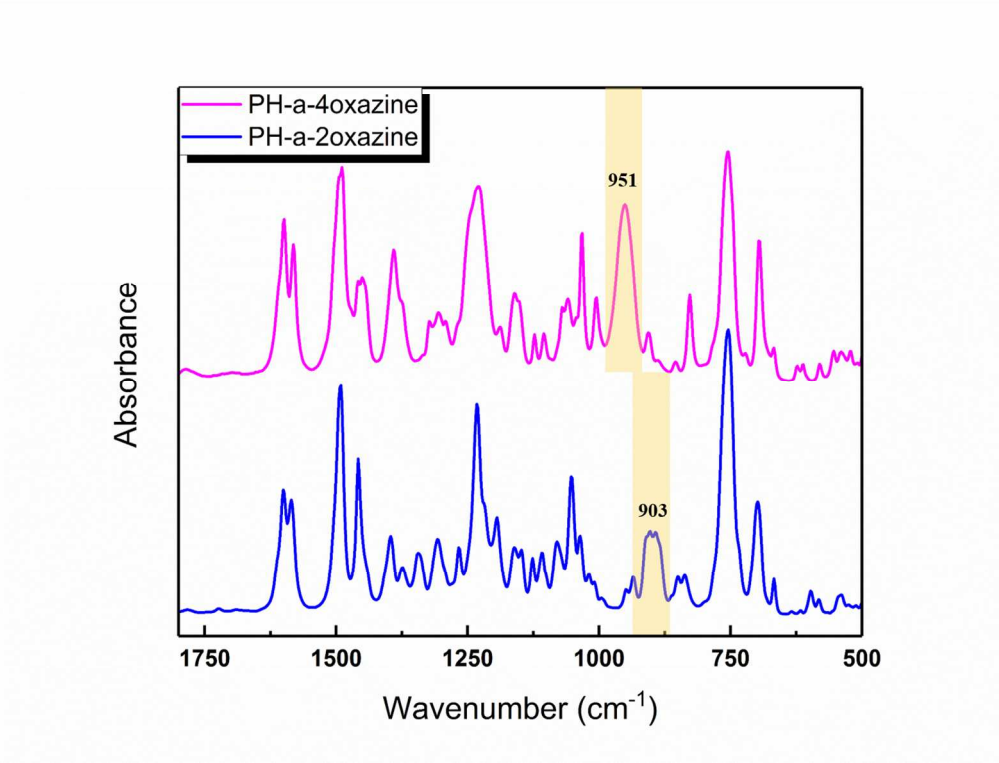

248x190mm (150 x 150 DPI)

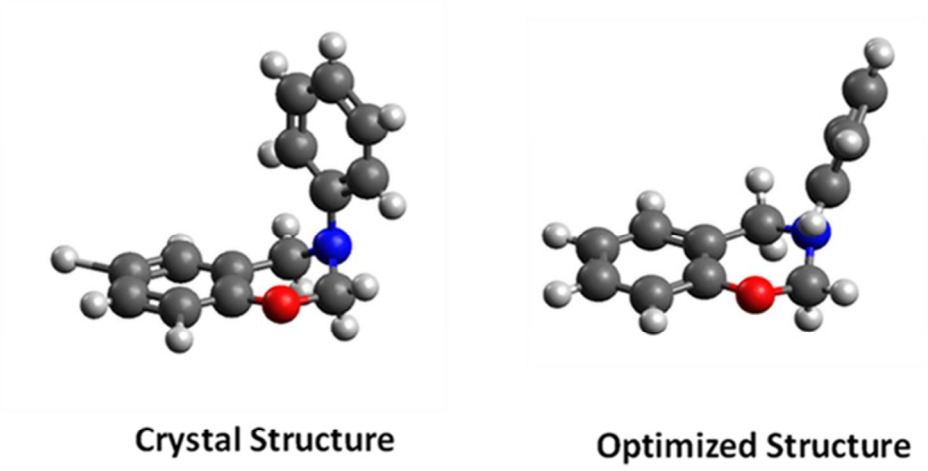

326x190mm (69 x 69 DPI)

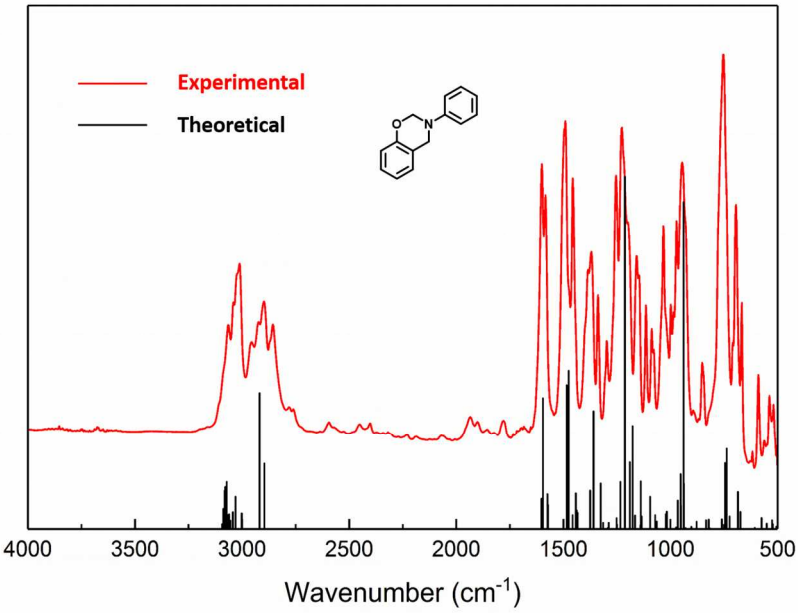

272x190mm (150 x 150 DPI)

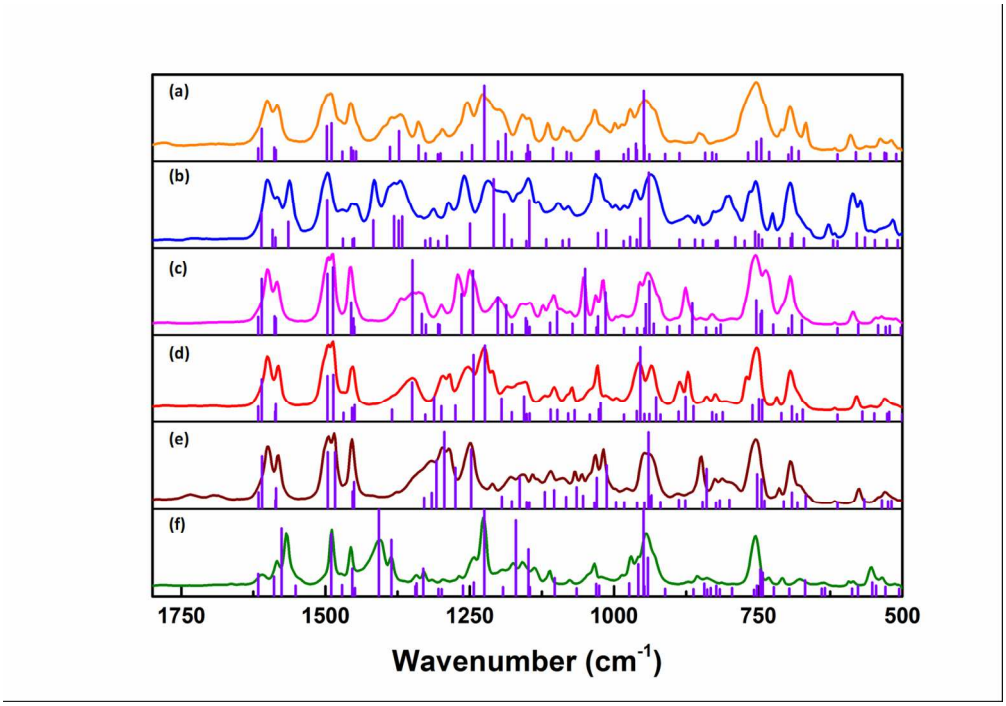

273x190mm (150 x 150 DPI)

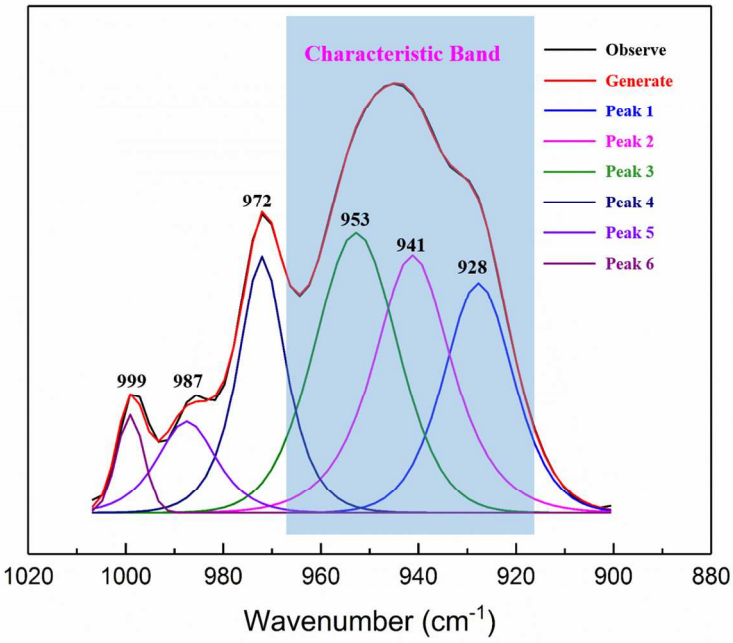

248x190mm (150 x 150 DPI)

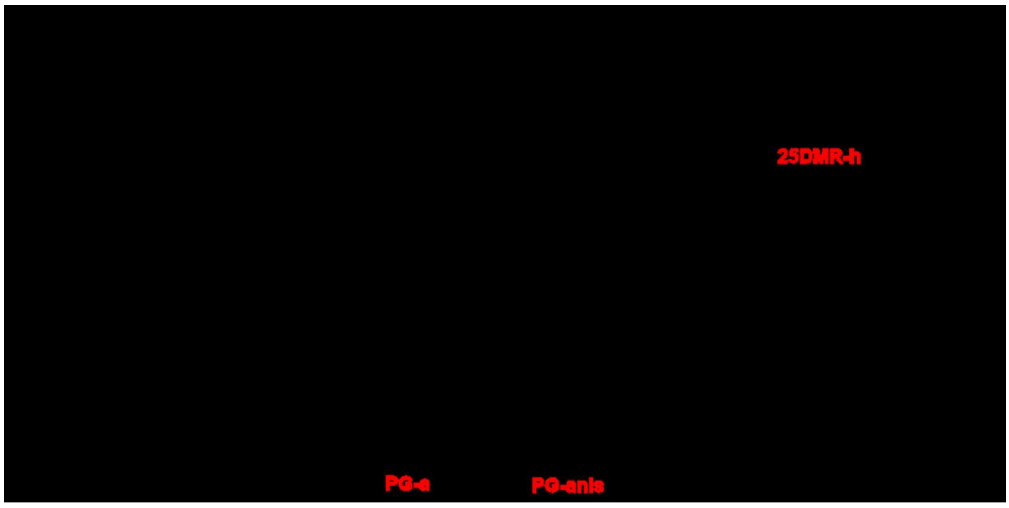

165x82mm (144 x 144 DPI)

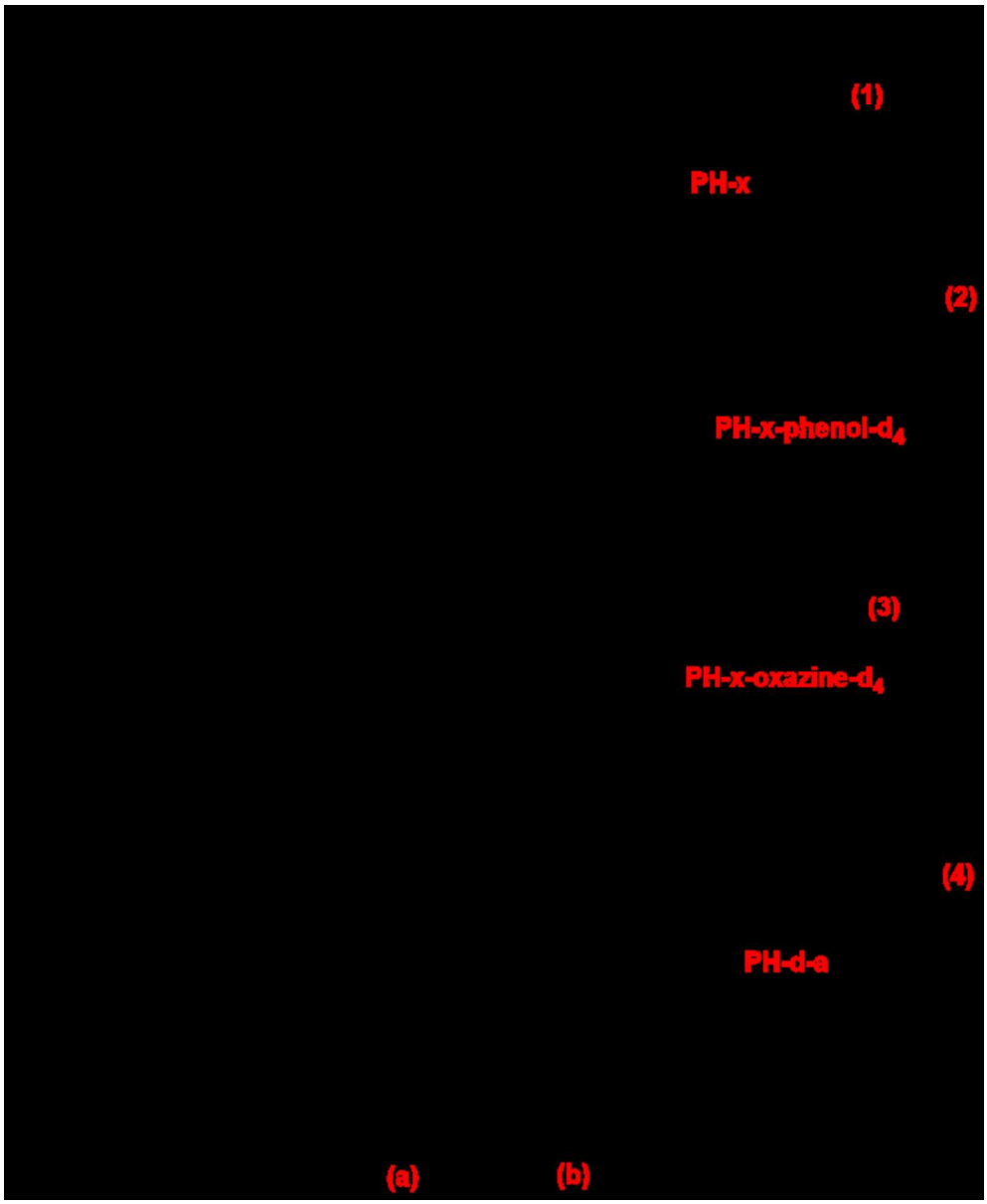

132x161mm (144 x 144 DPI)

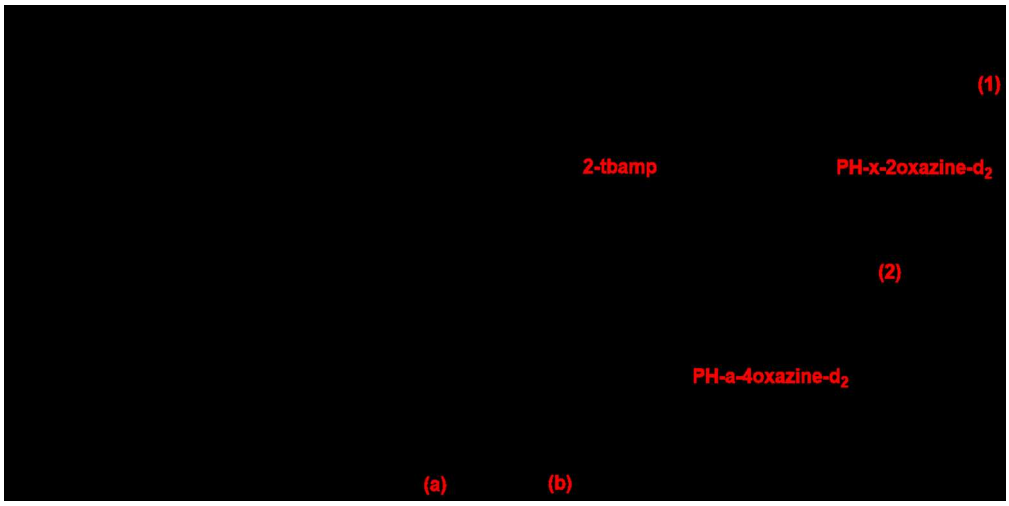

247x122mm (144 x 144 DPI)

122x36mm (144 x 144 DPI)

165x64mm (144 x 144 DPI)

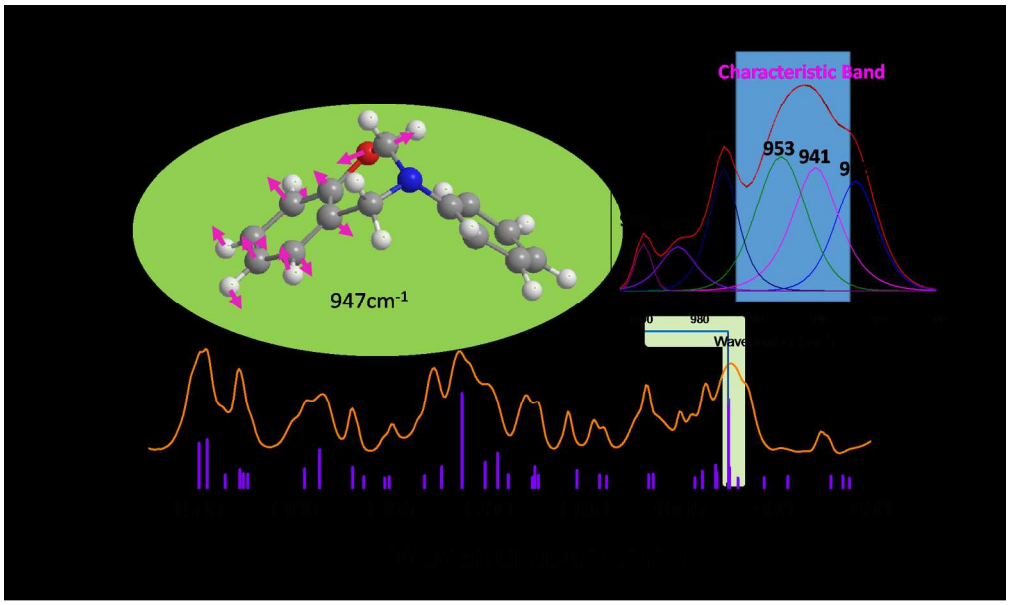

352x209mm (144 x 144 DPI)